

---

# PAC Learnability under Explanation-Preserving Graph Perturbations

---

Xu Zheng<sup>\*1</sup> Farhad Shirani<sup>\*1</sup> Tianchun Wang<sup>2</sup> Shouwei Gao<sup>1</sup> Wenqian Dong<sup>1</sup> Wei Cheng<sup>3</sup>  
 Dongsheng Luo<sup>1</sup>

## Abstract

Graphical models capture relations between entities in a wide range of applications including social networks, biology, and natural language processing, among others. Graph neural networks (GNN) are neural models that operate over graphs, enabling the model to leverage the complex relationships and dependencies in graph-structured data. A graph explanation is a subgraph which is an ‘almost sufficient’ statistic of the input graph with respect to its classification label. Consequently, the classification label is invariant, with high probability, to perturbations of graph edges not belonging to its explanation subgraph. This work considers two methods for leveraging such perturbation invariances in the design and training of GNNs. First, explanation-assisted learning rules are considered. It is shown that the sample complexity of explanation-assisted learning can be arbitrarily smaller than explanation-agnostic learning. Next, explanation-assisted data augmentation is considered, where the training set is enlarged by artificially producing new training samples via perturbation of the non-explanation edges in the original training set. It is shown that such data augmentation methods may improve performance if the augmented data is in-distribution, however, it may also lead to worse sample complexity compared to explanation-agnostic learning rules if the augmented data is out-of-distribution. Extensive empirical evaluations are provided to verify the theoretical analysis.

## 1. Introduction

Graphical models represent relations between entities in a wide range of applications such as social networks, biology, transportation systems, natural language processing,

<sup>\*</sup>Equal contribution <sup>1</sup>Florida International University  
<sup>2</sup>Pennsylvania State University <sup>3</sup>NEC Lab America.

and computer vision (Newman, 2018). Traditional machine learning approaches often struggle to effectively leverage the rich relational information encoded in graphs. To address this, and inspired by conventional deep learning methods, various graph neural network (GNN) architectures have been developed, such as methods based on convolutional neural networks (Defferrard et al., 2016; Kipf & Welling, 2017), recurrent neural networks (Li et al., 2016; Ruiz et al., 2020), and transformers (Yun et al., 2019; Rong et al., 2020). The application of machine learning solutions in critical domains such as autonomous vehicles, medical diagnostics, and financial systems has created an urgent need for explainable learning methods (Ying et al., 2019; Luo et al., 2020; Yuan et al., 2022; 2021). At a high level, explainability can be interpreted as identifying a subset of the input that significantly *influences* the model’s output. In the context of GNNs, this often translates to identifying an influential subgraph of the input graph. Recent works have proposed gradients-based (Pope et al., 2019b; Baldassarre & Azizpour, 2019a), perturbed-predictions-based (Ying et al., 2019; Luo et al., 2020; Yuan et al., 2021; Shan et al., 2021), and decomposition-based (Baldassarre & Azizpour, 2019a) methods for GNN explainability.

The notion of subgraph explainability is based on the intuitive assumption that the presence of certain structural patterns or motifs within the input graph plays a critical role in the model’s decision-making process (Ying et al., 2019; Luo et al., 2020; Yuan et al., 2021; Shan et al., 2021). Consequently, prior works have defined a graph explanation as a subgraph which is an *almost sufficient* statistic of the input graph with respect to the classification label. The design of many of the widely recognized GNN explanation algorithms such as GNNExplainer (Ying et al., 2019), PGExplainer (Luo et al., 2020), and GSAT (Miao et al., 2023), as well as fidelity measures such as  $Fid_+$ ,  $Fid_-$ , and  $Fid_\Delta$  (Pope et al., 2019b; Yuan et al., 2022) are based on the assumption that the presence or absence of the explanation subgraph in the input determines the output label with high accuracy, and hence perturbations of the non-explanation edges — graph edges which do not belong to the explanation subgraph — does not change the output label with high probability.

The invariance of the GNN output to perturbations of non-explanation edges resembles the transformation invariances

observed in various learning tasks on non-graphical data such as invariance to scaling and rotation in image classification tasks (Cohen & Welling, 2016; Bloem-Reddy et al., 2020; Chen et al., 2020; Shao et al., 2022). Such transformation invariances have been leveraged in both network architectural design and data augmentation in the context of image classification (Krizhevsky et al., 2012; He et al., 2016), electroencephalographic (EEG) classification (Krell & Kim, 2017), and radio modulation classification (Huang et al.), among other applications.

Analogous to the aforementioned prior works, which leverage various types of transformation invariances in non-graph learning applications to design learning mechanisms and data augmentation methods, in this work, we wish to study how one can leverage the invariance to perturbations of non-explanation edges for GNN architecture design and data augmentation. Particularly, we consider learning scenarios, where, in addition to labeled graph samples, each training sample is accompanied by its ground-truth explanation sub-graph. Such ground-truth explanations may be produced at the time that the training data is compiled. For example, in a dataset of labeled radiology scans, the most informative sections of each scan could be identified by the contributing physicians during the compilation phase of the training dataset. Alternatively, an estimate of the explanation can be produced by joint training of a GNN explainer and classifier using the original (unexplained) training data. Considering such scenarios, we introduce *explanation-assisted* learning rules and data augmentation methods.

Our main contributions are summarized in the following:

- To provide a rigorous formulation of the explanation-assisted graph learning problem and the associated sample complexity.
- To introduce the explanation-assisted empirical risk minimization (EA-ERM) learning rule, and derive its sample complexity, and to prove the optimality of the EA-ERM in terms of sample complexity. (Theorem 3.5)
- To show that the EA-ERM sample complexity can be arbitrarily smaller than the (explanation-agnostic) ERM sample complexity. (Example 3.4)
- To introduce explanation-assisted data augmentation mechanisms, and to provide a theoretical justification, along with an example, showing that while in some scenario such data augmentation mechanisms may improve performance, there also exist scenarios where they lead to worse sample complexity even compared to that of the explanation-agnostic learners. (Example 4.3)
- To provide an implementable class of explanation-assisted GNN mechanisms by building on the intuition from our theoretical analysis of EA-ERM. (Section 5)
- To provide empirical simulations verifying the improved performance of our explanation-assisted GNN architec-

tures when the necessary conditions in our theoretical derivations are satisfied; and to provide empirical simulations illustrating the diminished performance in scenarios not satisfying the necessary conditions. (Section 6)

## 2. Preliminaries

This section introduces the notation and some of the necessary background concepts used in the rest of the paper.

### 2.1. The Classification Problem

A random labeled graph  $G$  is parametrized by i) a vertex set  $\mathcal{V} = \{v_1, v_2, \dots, v_n\}$ , where  $n \in \mathbb{N}$ , ii) an edge set  $\mathcal{E} \subseteq \mathcal{V} \times \mathcal{V}$ , iii) a feature matrix  $\mathbf{X} \in \mathbb{R}^{n \times d}$ , where the  $i$ th row  $\mathbf{X}_i$  is the feature vector associated with  $v_i$  and  $d$  is the dimension of the feature vectors, iv) an adjacency matrix  $\mathbf{A} \in \{0, 1\}^{n \times n}$ , where  $A_{i,j} = \mathbb{1}((v_i, v_j) \in \mathcal{E})$ , and v) a label  $Y \in \mathcal{Y}$ , where  $\mathcal{Y}$  is a finite set. The graph parameters  $(Y, \mathbf{A}, \mathbf{X})$  are generated based on the joint distribution  $P_{Y, \mathbf{A}, \mathbf{X}}$ . The notation  $P_G$  and  $P_{Y, \mathbf{A}, \mathbf{X}}$  are used interchangeably. For a labeled graph  $G = (\mathcal{V}, \mathcal{E}; Y, \mathbf{X}, \mathbf{A})$ , the corresponding graph without label is denoted as  $\overline{G} = (\mathcal{V}, \mathcal{E}; \mathbf{X}, \mathbf{A})$ . The induced marginal distribution of  $\overline{G}$  is  $P_{\overline{G}}$  and its support is  $\overline{\mathcal{G}}$ . A classification scenario is completely characterized by  $P_G$ , consequently, in the rest of the paper, we refer to  $P_G$  as *the classification problem*.

**Definition 2.1 (Graph Classification).** *A graph classifier for a classification problem  $P_G$  is a function  $f : \overline{\mathcal{G}} \rightarrow \mathcal{Y}$ . Given  $\epsilon \in [0, 1]$ , the classifier is called  $\epsilon$ -accurate if  $P_G(f(\overline{G}) \neq Y) \leq \epsilon$ .*

### 2.2. Generic Learning Rules and ERM

A training set  $\mathcal{T}$  is a collection of labeled graphs. The elements of the training set are generated independently and according to  $P_G$ . A learning rule is a procedure which takes the training set  $\mathcal{T}$  as input, and outputs a graph classifier belonging to an underlying hypothesis class  $\mathcal{H}$ .

**Definition 2.2 (Generic Learning Rule).** *Let the hypothesis class  $\mathcal{H}$  be a collection of graph classifiers. A generic learning rule  $\mathbb{L} = (L_t)_{t \in \mathbb{N}}$  consists of a family of mappings  $L_t : \mathcal{T}_t \mapsto f(\cdot)$ , where the input  $\mathcal{T}_t = \{(\overline{G}_i, Y_i), i \in [t]\}$  is called the training set, and the output  $f : \overline{\mathcal{G}} \rightarrow \mathcal{Y}$  is a graph classifier belonging to the hypothesis class  $\mathcal{H}$ .*

The empirical risk minimization (ERM) learning rule is a subclass of generic learning rules defined below.

**Definition 2.3 (Empirical Risk Minimization).** *Given a hypothesis class  $\mathcal{H}$  and family of training sets  $\mathcal{T}_t = \{(\overline{G}_i, Y_i), i \in [t]\}, t \in \mathbb{N}$ , the learning rule  $\mathbb{L}_{ERM} =$*

<sup>1</sup>We use node and vertex interchangeably.

$(L_{ERM,t})_{t \in \mathbb{N}}$  is defined as:

$$L_{ERM,t}(\mathcal{T}_t) \triangleq \arg \min_{f(\cdot) \in \mathcal{H}} \frac{1}{t} \sum_{i=1}^t \mathbb{1}(f(\bar{G}_i) \neq Y_i), \quad t \in \mathbb{N}.$$

### 2.3. GNN Explainability

The objective in instance-level GNN explainability is to take a graph  $\bar{G}$  as input, and construct a subgraph  $\bar{G}_{exp}$  which is an (almost) sufficient statistic of the input graph with respect to its label. We adapt the formalization introduced in (Zheng et al., 2023) which is summarized in the following.

**Definition 2.4 (Explanation Function).** Given a classification problem  $P_G$ , an explanation function (explainer) is a mapping  $\Psi : \bar{G} \rightarrow 2^{\mathcal{V}} \times 2^{\mathcal{E}}$ , such that

$$\Psi(\bar{G}) = (\mathcal{V}_{exp}, \mathcal{E}_{exp}), \bar{G} \in \bar{\mathcal{G}},$$

where  $\mathcal{V}_{exp} \subseteq \mathcal{V}$ ,  $\mathcal{E}_{exp} = (\mathcal{V}_{exp} \times \mathcal{V}_{exp}) \cap \mathcal{E}$ , and  $\mathcal{V}$  and  $\mathcal{E}$  are the vertex set and edge set of  $\bar{G}$ , respectively. For a given pair of parameters  $\kappa \in [0, 1]$  and  $s \in \mathbb{N}$ , the explainer  $\Psi(\cdot)$  is called an  $(s, \kappa)$ -explainer if:

$$i) \quad I(Y; \bar{G} | \mathbb{1}_{\Psi(\bar{G})}) \leq \kappa, \quad ii) \quad \mathbb{E}_G(|\mathcal{E}_{exp}|) \leq s,$$

where we have defined

$$I(Y; \bar{G} | \mathbb{1}_{\Psi(\bar{G})}) \triangleq \sum_{g_{exp}} P_{\Psi(\bar{G})}(g_{exp}) \sum_{y, \bar{g}} P_{Y, \bar{G}}(y, \bar{g} | g_{exp} \subseteq \bar{G}) \times \log \frac{P_{Y, \bar{G}}(y, \bar{g} | g_{exp} \subseteq \bar{G})}{P_Y(y | g_{exp} \subseteq \bar{G}) P_{\bar{G}}(\bar{g} | g_{exp} \subseteq \bar{G})}.$$

If such an explainer exists, the classification problem is said to be  $(s, \kappa)$ -explainable.

To keep the analysis tractable, for all explanation functions considered in our theoretical analysis, we assume that:

$$\text{Condition 1: } \forall \bar{g}, \bar{g}' \in \bar{\mathcal{G}} : \Psi(\bar{g}) \subseteq \bar{g}' \Rightarrow \Psi(\bar{g}') = \Psi(\bar{g}). \quad (1)$$

This implies that  $I(Y; \bar{G} | \mathbb{1}_{\Psi(\bar{G})}) = I(Y; \bar{G} | \Psi(\bar{G}))$ . The condition holds for the ground-truth explanation in various datasets studied in the explainability literature such as BA-2motifs, Tree-Cycles, Tree-Grid, and MUTAG datasets. For a more complete background discussion of Definition 2.4 and Condition 1, and its connections with other widely used explainability measures such as graph information bottleneck (GIB), please refer to (Zheng et al., 2023).

### 2.4. Explanation-Assisted Learning Rules

We define explanation-assisted learning rules and their associated sample complexity as follows.

**Definition 2.5 (Explanation-Assisted Learning Rule).** Given a hypothesis class  $\mathcal{H}$ , an explanation-assisted learning rule  $\mathbb{L}_{EA} = (L_{EA,t})_{t \in \mathbb{N}}$  consists of a family of mappings  $L_{EA,t} : (\mathcal{T}_t, \Psi|_{\mathcal{T}_t}(\cdot)) \mapsto f(\cdot)$ , where  $\mathcal{T}_t, t \in \mathbb{N}$  is the

training set,  $\Psi(\cdot)$  is an explanation function, and  $\Psi|_{\mathcal{T}_t}(\cdot)$  is its restriction to the training set.

To define the sample complexity of explanation-assisted learning rules over *explainable* classification problems, we first introduce the class of perturbation-invariant classification problems. In the subsequent sections, we quantify the relation between perturbation-invariance and explainability (see Proposition 3.1).

**Definition 2.6 (Perturbation-Invariant Classification Problem).** Given an explainer  $\Psi(\cdot)$  and parameters  $\zeta \in [0, 1]$ , a classification problem  $P_G$  is  $(\Psi, \zeta)$ -invariant if

$$\sum_{g_{exp}} P(\Psi(\bar{G}) = g_{exp}) \times P(Y_{\bar{G}'} \neq Y_{\bar{G}''} | \Psi(\bar{G}') = \Psi(\bar{G}'') = g_{exp}) \leq \zeta,$$

where  $Y_{\bar{G}'}$  and  $Y_{\bar{G}''}$  are the labels associated with  $\bar{G}'$  and  $\bar{G}''$ , respectively, and the labeled graphs  $\bar{G}, \bar{G}', \bar{G}''$  are generated independently and according to  $P_{\bar{G}}$

As shown in our empirical analysis, the perturbation-invariant property can be empirically observed in many of the graph classification datasets considered in the literature, such as the BA2-Motifs dataset (Luo et al., 2020), where the graph label is completely determined by the presence of specific motifs, and does not change with perturbations of edges in the graph that are not part of the motifs. Similarly, in the Mutag dataset, labels indicating mutagenicity are associated with various motifs such as aromatic nitro groups, polycyclic aromatic hydrocarbons, and alkylating agents (Debnath et al., 1991). We define sample complexity of explanation-assisted learning rules over perturbation invariant classification problems in the following.

**Definition 2.7 (Explanation-Assisted Sample Complexity).** For any  $\epsilon, \delta, \zeta \in (0, 1)$ , the sample complexity of  $(\epsilon, \delta, \zeta)$ -PAC learning of  $\mathcal{H}$  with respect to explanation function  $\Psi(\cdot)$ , denoted by  $m_{EA}(\epsilon, \delta, \zeta; \mathcal{H}, \Psi)$ , is defined as the smallest  $m \in \mathbb{N}$  for which there exists an explanation-assisted learning rule  $\mathbb{L}$  such that, for every  $(\Psi, \zeta)$ -invariant classification problem  $P_G$ , we have:

$$P \left( \text{err}_{P_G}(\mathbb{L}(\mathcal{T})) \leq \inf_{f \in \mathcal{H}} \text{err}_{P_G}(f) + \epsilon \right) \geq 1 - \delta,$$

where we have defined  $\text{err}_{P_G}(f)$  as the statistical error of  $f(\cdot)$  on  $P_G$ , and probability is evaluated with respect to the training set  $\mathcal{T}$ . If no such  $m$  exists, then we say the sample complexity is infinite.

## 3. PAC Learnability of Explanation-Assisted Learners

In this section, we introduce the explanation-assisted ERM (EA-ERM), characterize its sample complexity, and prove

its optimality. We provide an example, where this sample complexity can be arbitrarily smaller than the standard explanation-agnostic sample complexity achieved by ERM. We conclude that for explainable classification problems there may be significant benefits in using explanation-assisted learning rules, in terms of size of the training set required to achieve a specific error probability. This is further verified via empirical analysis in the subsequent sections.

As a first step, the following proposition provides sufficient conditions for perturbation-invariance of a classification problem in terms of its explainability parameters and its Bayes error probability.

**Proposition 3.1 (Perturbation Invariance and Explainability).** *Let  $\zeta \in [0, 1]$ . There exist  $\bar{\kappa}, \bar{\epsilon} > 0, s \in \mathbb{N}$ , such that for all  $\kappa \leq \bar{\kappa}$  and  $\epsilon \leq \bar{\epsilon}$ , any  $(\kappa, s)$ -explainable classification problem  $P_G$  with Bayes error  $\epsilon$  is  $(\Psi, \zeta)$ -invariant, where  $\Psi(\cdot)$  is a  $(\kappa, s)$ -explanation function for  $P_G$ .*

The proof is provided in Appendix A.1.

The notion of perturbation invariance is analogous to transformation invariances, such as rotation and scaling invariances, observed in image classification. Prior works on sequential data have shown that in those contexts invariance-aware learning rules can achieve improved sample complexity, e.g., (Shao et al., 2022). Building on this, we define EA-ERM as follows.

**Definition 3.2 (Explanation-Assisted ERM (EA-ERM)).** *Given a hypothesis class  $\mathcal{H}$ , family of training sets  $\mathcal{T}_t, t \in \mathbb{N}$ , and explanation function  $\Psi(\cdot)$ , the learning rule  $L_{EA-ERM} = (L_{EA-ERM,t})_{t \in \mathbb{N}}$  is defined as:*

$$\begin{aligned} L_{EA-ERM,t} &\triangleq \tilde{f}_t(\cdot), \quad t \in \mathbb{N} \\ \tilde{f}_t(\bar{G}) &\triangleq \begin{cases} Y_{exp} & \exists i \in [t]: \Psi(\bar{G}_i) \subseteq \bar{G}, \\ f_t(\bar{G}) & \text{Otherwise} \end{cases}, \quad (2) \\ f_t(\cdot) &\triangleq L_{ERM,t}(\mathcal{T}_t), \end{aligned}$$

where  $Y_{exp}$  is chosen randomly and uniformly from the set  $\{Y_i | \Psi(\bar{G}_i) \subseteq \bar{G}, i \in [t]\}$ .

Note that Definition 3.2 implies a two-step learning procedure. First, given a training set  $\mathcal{T}_t$ , a classifier  $f_t(\cdot)$  is trained by applying the ERM learning rule  $L_{ERM,t}$ . Then,  $\tilde{f}_t(\cdot)$  is constructed from  $f_t(\cdot)$  using equation 2. This step ensures that the output of the classifier is the same for all explanation-preserving perturbations of the training samples. The second step was shown to be necessary to achieve improved sample complexity in (Shao et al., 2022) in the context of transformation invariances.

**Definition 3.3 (Explanation-Assisted VC Dimension).** *Given an explanation function  $\Psi(\cdot)$  and hypothesis class  $\mathcal{H}$ , the explanation-assisted VC dimension  $VC_{EA}(\mathcal{H}, \Psi)$  is defined as the largest integer  $k$  for which there exists a*

*collections of labeled graphs  $\mathcal{G} = \{\bar{g}_1, \bar{g}_2, \dots, \bar{g}_k\}$  such that  $\Psi(\bar{g}_i) \neq \Psi(\bar{g}_j)$  for all  $i \neq j$ , and every labeling of  $\mathcal{G}$  is realized by the hypothesis class  $\mathcal{H}$ .*

Let us define  $\mathbf{I}(\bar{G}) = \bar{G}$  as the identity function. We call  $VC(\mathcal{H}) \triangleq VC_{EA}(\mathcal{H}, \mathbf{I})$  the *standard* VC dimension as it aligns with the notion of VC dimension considered in traditional PAC learnability analysis. The following provides a simple example, in which the standard VC dimension,  $VC(\mathcal{H})$ , can be arbitrarily larger than the explanation-assisted VC dimension  $VC_{EA}(\mathcal{H}, \Psi(\cdot))$ .

**Example 3.4.** *Let  $C_i, i \in \mathbb{N}$  denote the single-cycle graph with  $i$  vertices, where the vertex set is  $\mathcal{V}_i = [i]$  and the edge set is  $\mathcal{E}_i = \{(j, j+1), j \in [i-1]\} \cup \{(1, i)\}$ . We construct a binary classification problem as follows. Let the graphs associated with label zero belong to the collection  $\mathcal{B}_0 = \{C_i \cup C_3, i > 5\}$  and those associated with label one belong to  $\mathcal{B}_1 = \{C_i \cup C_4, i > 5\}$ . Let*

$$\Psi(\bar{G}) = \begin{cases} C_3 & \text{if } \bar{G} \in \mathcal{B}_0 \\ C_4 & \text{otherwise} \end{cases}.$$

*Clearly,  $\zeta = 0$  in this case. Let  $P_Y(\cdot)$  be Bernoulli with parameter  $\frac{1}{2}$ , so that the two labels are equally likely, and assume that for a given label  $Y = y$ , the graphs belonging to  $\mathcal{B}_y$  are equally likely, i.e.,  $P_{\bar{G}|Y}(\cdot|y)$  is uniform. Let  $\mathcal{H}$  consist of all possible classifiers on the set  $\mathcal{B}_0 \cup \mathcal{B}_1$ . So that  $VC(\mathcal{H}) = \infty$ . It is straightforward to see that  $VC(\mathcal{H}, \Psi(\cdot)) = 2$  since there are only two explanation graphs, namely  $C_3$  and  $C_4$ .*

Next, we show that explanation-assisted learning rules achieve sample complexity equal to  $VC_{EA}(\mathcal{H}, \Psi(\cdot))$  as opposed to  $VC(\mathcal{H})$  achieved by generic learning rules.

**Theorem 3.5 (Sample Complexity of Explainable Tasks).** *Let  $\epsilon, \delta \in (0, 1)$  and  $\zeta \leq \frac{\epsilon}{32}$ . For any hypothesis class  $\mathcal{H}$  and explanation function  $\Psi(\cdot)$ , the following holds:*

$$m_{EA}(\epsilon, \delta, \zeta; \mathcal{H}, \Psi) = O\left(\frac{d}{\epsilon^2} \log^2 d + \frac{1}{\epsilon^2} \ln\left(\frac{1}{\delta}\right)\right),$$

where we have defined  $d \triangleq VC_{EA}(\mathcal{H}, \Psi(\cdot))$ .

The proof is provided in Appendix A.2.

## 4. PAC Learnability of Explanation-Assisted Dataset Augmentation

In the previous section, we showed that explanation-assisted learning rules outperform generic explanation-agnostic learning rules in terms of sample complexity. This suggests that if explanation subgraphs associated with each of the training samples are accessible, then an optimal learning rule should utilize those samples to learn the classifi-

cation rule. One method for utilizing the explanation subgraphs is to perform data augmentation, by producing artificial training inputs with the same explanation subgraphs, and perturbed non-explanation edges. In this section, we show through a simple example that this approach may lead to worse sample complexity even compared to generic explanation-agnostic learning rules. This phenomenon is also observed in our empirical observations in the subsequent sections. As a result, while the explanations may assist in designing the learning rule, it is not necessarily helpful to use them to enlarge the training set by data augmentation without distinguishing explicitly between the artificially synthesized training elements and the original training elements. To this end, we define the data-augmentation learning rules and data-augmentation ERM (DA-ERM) as follows.

**Definition 4.1 (Explanation-Preserving Perturbation).** Consider a classification problem  $P_G$ , an explanation function  $\Psi(\cdot)$ , and parameter  $\gamma > 0$ . An explanation-preserving perturbation with parameter  $\gamma$  is a mapping  $S^\gamma(\cdot)$  operating on  $\overline{G}$ , where<sup>2</sup>

$$S^\gamma(\overline{G}) \triangleq \{\overline{G}' \mid \Psi(\overline{G}) \subseteq \overline{G}', |\mathcal{E}\Delta\mathcal{E}'| \leq \gamma|\mathcal{E}|\},$$

$\mathcal{E}$  and  $\mathcal{E}'$  are the edge sets of  $\overline{G}$  and  $\overline{G}'$ , respectively, and  $\Delta$  denotes the symmetric difference.

**Definition 4.2 (Data-Augmentation Learning Rule).** Given an explainer  $\Psi(\cdot)$ , a hypothesis class  $\mathcal{H}$ , and a learning rule  $\mathsf{L} = (L_t)_{t \in \mathbb{N}}$ , a data-augmentation learning rule  $\mathsf{L}_{exp} = (L_{exp,t})_{t \in \mathbb{N}}$  consists of a family of mappings

$$L_{exp,t} : \mathcal{T}_t \mapsto \tilde{f}(\cdot),$$

where,

$$\tilde{f}(\overline{G}) = \begin{cases} Y_{exp} & \exists i \in [t] : \Psi(\overline{G}_i) \subseteq \overline{G}, \\ f(\overline{G}) & \text{Otherwise} \end{cases}, \quad (3)$$

$Y_{exp}$  is chosen randomly and uniformly from the set  $\{Y_i \mid \Psi(\overline{G}_i) \subseteq \overline{G}, i \in [t]\}$ ,  $f(\cdot) \triangleq L_t(\mathcal{T}_{aug,t})$ , and we have defined the augmented training set as

$$\mathcal{T}_{aug,t} \triangleq \mathcal{T}_t \cup \left( \bigcup_{(\overline{G}, Y) \in \mathcal{T}_t} \{(\overline{G}', Y) \mid \overline{G}' \in S^\gamma(\overline{G})\} \right).$$

The learning rule is a DA-ERM learning rule if  $\mathsf{L} = \mathsf{L}_{ERM}$ .

For  $\gamma = 0$ , DA-ERM is the same as EA-ERM and there is no data augmentation. The following example shows that in general, for  $\gamma > 0$ , DA-ERM may have worse sample complexity than the explanation-agnostic ERM.

<sup>2</sup> $S^\gamma(\overline{G})$  is defined with respect to  $\Psi(\cdot)$ . This dependence is not made explicit in our notation to avoid clutter.

**Example 4.3.** Consider the hypothesis class  $\mathcal{H}$  which consists of all classifiers that classify their input only based on the number of edges in the graph. That is,

$$\mathcal{H} = \{f(\cdot) \mid \forall \overline{G}, \overline{G}' : |\overline{G}| = |\overline{G}'| \rightarrow f(\overline{G}) = f(\overline{G}')\}.$$

Furthermore, let us consider the following binary classification problem. Let  $P_Y(\cdot)$  be a binary symmetric distribution, i.e.,  $P_Y(0) = P_Y(1) = \frac{1}{2}$ . Let the graphs associated with label 0 consist of the collection

$$\mathcal{B}_0 = \{\overline{G} \mid |\overline{G}| = n, \exists i \in [n] : C_i \subseteq \overline{G} \text{ and } \nexists j \subseteq [n] : D_j \subseteq \overline{G}\},$$

where  $n > 10$  is a fixed number,  $C_i, i \in [n]$  denotes a cycle of size  $i$ , and  $D_i$  denotes a star of size  $i$ , where a star is a subgraph where all vertices are connected to a specific vertex called the center, and there are no edges between the rest of the vertices. Thus,  $\mathcal{B}_0$  consists of all graphs with exactly  $n$  edges that contain at least one cycle but no stars. Similarly, let the graphs associated with label 1 be given by

$$\mathcal{B}_1 = \{\overline{G} \mid |\overline{G}| = n + 1, \nexists i \in [n + 1] : C_i \subseteq \overline{G} \text{ and } \exists j \in [n + 1] : D_j \subseteq \overline{G}\}.$$

That is,  $\mathcal{B}_1$  consists of all graphs with exactly  $n + 1$  edges that do not contain a cycle but contain a star. Let  $\gamma = \frac{1}{n}$ , and define

$$\Psi(\overline{G}) \triangleq \begin{cases} C_i & \text{if } \exists i : C_i \subseteq \overline{G}, \\ D_i & \text{if } \exists i : D_i \subseteq \overline{G}, \end{cases}$$

Clearly  $\zeta = 0$  in this case. Then, it is straightforward to see that ERM and EA-ERM both achieve zero error after observing at least one sample per label since all graphs of size  $n$  have label 0 and all graphs of size  $n + 1$  have label 1, and the hypothesis class decides based only on the number of edges. On the other hand, for DA-ERM to achieve zero error it needs to observe all possible explanation outputs, as it cannot distinguish between the augmented elements of  $\mathcal{B}_0$  and the original elements of  $\mathcal{B}_1$  and vice versa since they may have the same number of edges. Thus, data augmentation yields infinite sample complexity, whereas ERM and EA-ERM have sample complexity equal to two.

The issue illustrated in the previous example appears to be a fundamental issue. To explain further, note that DA-ERM empirically minimizes the risk over the augmented dataset. If the elements of the augmented dataset are in-distribution with respect to  $P_G$ , this also guarantees that the risk is minimized with respect to the original dataset, hence achieving similar performance as that of EA-ERM. However, if the elements of the augmented dataset are out-of-distribution with respect to  $P_G$ , then it may be the case that the output of DA-ERM performs well on the out-of-distribution elements, but has high error on the in-distribution elements

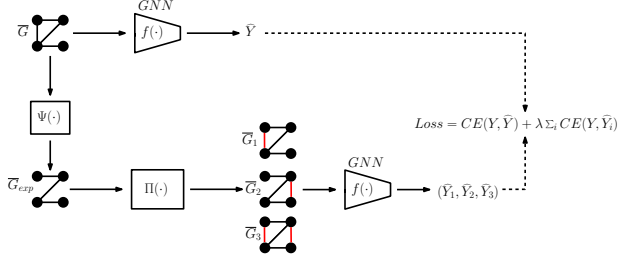


Figure 1. Given training sample  $(\bar{G}, Y)$ , the explanation subgraph  $\bar{G}_{exp} = \Psi(\bar{G})$  is produced. Then,  $\Pi(\bar{G}_{exp})$  produces the explanation-preserving perturbations  $\bar{G}_i$ .  $\hat{Y}$  and  $\hat{Y}_i$  are produced by passing the original and perturbed graphs through  $f(\cdot)$ , respectively. The loss is defined as a weighted sum of the classification loss of original and perturbed graphs.

(which are dominated by the out-of-distribution elements). Hence, DA-ERM may achieve high error probability on the original data distribution. This is exactly the phenomenon that is observed in the previous example. We show this phenomenon empirically and further explain it in our empirical evaluations in the subsequent sections.

## 5. Explanation-Assisted GNN Architectures

In Section 3, we showed that the sample complexity for EA-ERM can be arbitrarily smaller than that of standard explanation-agnostic learning methods. However, EA-ERM faces two major issues: i) empirical risk minimization across the hypothesis class is impractical for real-world applications; ii) the EA-ERM approach requires an exhaustive search over all explanation subgraphs in the training set to verify if any are a subgraph of the input. The first issue can be addressed by developing efficient learning algorithms that approximate the risk-minimizing classifier similar to traditional learning approaches. However, the second problem is intrinsic to the design of EA-ERM.

An alternative solution, explored in Section 4, is the data augmentation method. This method enlarges the training set by generating new samples through explanation-preserving perturbations of existing training samples. However, we showed through an example that if the learning algorithm does not distinguish between these artificially generated augmented samples and the original training samples, it could lead to worse performance even compared to conventional explanation-agnostic learning methods. Building on the theoretical observations of previous sections, in this section, we introduce a practically implementable explanation-assisted GNN architecture and training procedure. As shown in Figure 1, given a labeled training sample  $(\bar{G}, Y)$  and explanation function  $\Psi(\cdot)$ , we first compute an explanation subgraph  $\bar{G}_{exp} = \Psi(\bar{G})$ . Then, we use an explanation-preserving, non-parametric perturbation operator  $\Pi(\cdot)$  to produce perturbations  $\bar{G}_i$  of the original input graph  $\bar{G}$ ,

### Algorithm 1 Explanation-Assisted Training Algorithm

---

```

1: Input: Training set  $\mathcal{T}$ , balancing coefficient  $\lambda$ , GNN pre-train
   epoch  $e_w$ , train epoch  $e_s$ , sampling number  $M$ 
2: Output: Trained model  $f$ 
3: Initiate  $f, \Psi, j = 0$ 
4: for  $j \leq e_w$  do
5:   Update  $f$  via  $\mathbb{E}_{\mathcal{T}}(CE(Y, f(\bar{G})))$ 
6:    $j = j + 1$ 
7: end for
8: Initiate empty set  $\mathcal{T}'$ 
9: for each  $(\bar{G}, Y) \in \mathcal{T}$  do
10:   $\bar{G}_{exp} = \Psi(\bar{G})$ 
11:  for  $m$  in  $[1, 2, \dots, M]$  do
12:     $\mathcal{T}' = \mathcal{T}' + \{(\Pi(\bar{G}_{exp}), Y)\}$ .
13:  end for
14: end for
15: Initialize  $f, j = 0$ 
16: for  $j \leq e_s$  do
17:  Train  $f$  with  $\mathbb{E}_{\mathcal{T}}(CE(Y, f(\bar{G}))) + \lambda \mathbb{E}_{\{\mathcal{T}'\}}(CE(Y, f(\bar{G})))$ 
18:   $j = j + 1$ 
19: end for
    
```

---

such that  $\bar{G}_{exp} \subseteq \bar{G}_i$ . Then,  $\bar{G}$  and  $\bar{G}_i$  are passed through the GNN  $f(\cdot)$  to produce the output labels  $\hat{Y}$  and  $\hat{Y}_i$ , respectively. The loss is defined as:

$$Loss = CE(Y, \hat{Y}) + \lambda \sum_i CE(Y, \hat{Y}_i). \quad (4)$$

As shown in Section 4, if the perturbed graphs are out-of-distribution with respect to the input graph distribution, then the performance may be worse than explanation-agnostic methods. This is addressed in two ways in our training procedure. First, we follow an existing work to implement the perturbation function  $\Pi(\cdot)$  which randomly removes a small number of non-explanation edges (Zheng et al., 2023) (Algorithm 2). As shown in previous studies, this method is effective in generating in-distribution graphs. Second, to further alleviate the negative effects of out-of-distributed augmentations, we choose the hyperparameter  $\lambda$  (in Eq. 4) small enough, so that the loss on the (potentially out-of-distribution) augmented data does not dominate the loss on the original data.

It should be noted that the ground-truth explanation  $\Psi(\bar{G})$  may not be available beforehand in real-world applications. In such scenarios, we pre-train the graph classifier  $f(\cdot)$  and  $\Psi(\cdot)$ . This two-step training procedure is described in Algorithm 1. The proposed method is a general framework that can be employed for training various GNN architectures and explainers, such as GIN (Xu et al., 2019), PNA (Corso et al., 2020), GNNExplainer (Ying et al., 2019) and PGExplainer (Luo et al., 2020).

## 6. Empirical Verification

This section empirically verifies our theoretical analysis and demonstrates the effectiveness of the proposed method.

**Algorithm 2** In-distributed explanation-preserving perturbation function  $\Pi(\cdot)$

- 1: **Input:** a graph  $\overline{G}$ , explainer  $\Psi(\cdot)$ , hyper-parameter  $\alpha_1$ .
- 2:  $\overline{G}^c = \overline{G} - \Psi(\overline{G})$
- 3:  $E_{\alpha_1}(\overline{G}^c) = \text{sample } \alpha_1 \text{ edges from } \overline{G}^c$
- 4: **Return**  $E_{\alpha_1}(\overline{G}^c) + \Psi(\overline{G})$

Table 1. Performance comparisons with 3-layer GNNs trained on 50 samples. The metric is classification accuracy. The best results are shown in bold font and the second best ones are underlined.

| Dataset           | MUTAG           | Benzene         | Fluoride        | Alkane          | D&D             | PROTEINS        |
|-------------------|-----------------|-----------------|-----------------|-----------------|-----------------|-----------------|
|                   | GCN             |                 |                 |                 |                 |                 |
| Vanilla           | 84.3±3.2        | 73.9±5.2        | 62.1±4.3        | 93.7±3.2        | 63.2±6.6        | 68.1±6.1        |
| EI                | 85.6±2.0        | 75.3±5.1        | 59.3±3.2        | 92.2±4.9        | 63.6±6.2        | 69.6±4.0        |
| ED                | 84.7±3.4        | 73.2±4.1        | 58.4±3.7        | 94.4±1.8        | 64.0±6.0        | 70.0±4.0        |
| ND                | 83.6±3.5        | 74.0±3.8        | 58.7±3.0        | 92.7±3.4        | 65.2±4.2        | 68.8±3.3        |
| FD                | 84.7±3.4        | 75.2±4.8        | 57.6±3.6        | 93.8±3.1        | 62.5±3.3        | 68.6±3.8        |
| Mixup             | 67.4±3.2        | 53.9±1.9        | 52.5±1.5        | 64.3±0.7        | 56.0±1.9        | 60.8±2.9        |
| Aug <sub>GE</sub> | 87.2±1.4        | 76.2±1.3        | <b>66.6±3.4</b> | <u>96.3±1.3</u> | 66.1±5.1        | 70.4±5.9        |
| Aug <sub>PE</sub> | <b>87.2±2.6</b> | <b>76.5±0.8</b> | <u>65.3±5.0</u> | <b>96.4±1.1</b> | <b>67.7±4.3</b> | <b>71.2±6.3</b> |
|                   | GIN             |                 |                 |                 |                 |                 |
| Vanilla           | 82.5±3.7        | 67.5±5.9        | 68.6±5.2        | 85.1±10.3       | 65.1±4.3        | 66.5±4.0        |
| EI                | 82.8±3.2        | 71.6±2.8        | 66.8±4.0        | 87.5±10.3       | 64.7±5.4        | 65.5±5.8        |
| ED                | 81.6±3.7        | 70.5±4.3        | 62.9±5.1        | 90.3±6.4        | 66.7±3.8        | 62.7±5.3        |
| ND                | 82.2±4.0        | 71.3±2.7        | 64.9±4.6        | 88.9±7.0        | 66.7±2.9        | 65.6±5.4        |
| FD                | 82.7±2.9        | 70.7±2.8        | 67.6±5.1        | 83.1±11.7       | 68.2±4.3        | 65.6±5.0        |
| Mixup             | 74.5±1.6        | 59.0±3.4        | 51.6±2.6        | 65.8±4.1        | 58.6±3.5        | 62.2±2.9        |
| Aug <sub>GE</sub> | 86.0±2.4        | <b>75.4±0.8</b> | <u>76.3±2.1</u> | <b>94.9±1.1</b> | <b>69.3±5.2</b> | <b>68.5±5.9</b> |
| Aug <sub>PE</sub> | <b>86.9±1.8</b> | <u>75.4±1.0</u> | <b>76.5±1.7</b> | <u>94.8±1.1</u> | <u>67.4±2.8</u> | 68.1±5.5        |

A benchmark synthetic dataset, BA-2motifs (Luo et al., 2020), and five real-world datasets, MUTAG (Luo et al., 2020), Benzene, Fluoride, Alkane (Agarwal et al., 2023), D&D (Dobson & Doig, 2003) and PROTEINS (Dobson & Doig, 2003; Borgwardt et al., 2005) are utilized in our empirical studies. We consider three representative GNN models: Graph Convolutional Network (GCN), Graph Isomorphism Network (GIN), and Principal Neighbourhood Aggregation (PNA) (Corso et al., 2020). Full experimental setups are shown in the Appendix B.

### 6.1. Comparison to Baseline Data Augmentations.

With this set of experiments, we aim to verify the effectiveness of our explanation-assisted graph learning algorithm.

**Experimental Design.** In Section 3, we evaluate the sample complexity of explanation-assisted learning rules and quantify the resulting improvements over explanation-agnostic learning rules. We consider 3 GNN layers in each model. For each dataset, we randomly sample 50 labeled graphs for training and 10% graphs for testing. Experiments with smaller training sizes and lightweight GNN models can be found in Appendix C.5 and C.6, respectively. We compare with representative structure-oriented augmentations, Edge Inserting (EI), Edge Dropping (ED), Node Dropping (ND), and Feature Dropping (FD) (Ding et al., 2022). Re-

cently, mixup operations have been introduced in the graph domain for data augmentation, such as  $M$ -mixup (Wang et al., 2021b) and  $G$ -mixup (Han et al., 2022). However,  $M$ -mixup is operating on the embedding space and cannot be fairly compared, and  $G$ -mixup does not apply to graphs with node type/features. Instead, we use a normal Mixup as another baseline. For the explainer function  $\Psi(\cdot)$  in our method, we consider two representative explainers, GNExplainer (Ying et al., 2019) and PGExplainer (Luo et al., 2020), whose corresponding augmentations are denoted by Aug<sub>GE</sub> and Aug<sub>PE</sub>, respectively. More comprehensive results on different settings and full experimental results are shown in Appendix C.

**Experimental Results.** From Tables 1 and 3 (in the Appendix), we have the following observations. First, our explanation-assisted learning methods consistently outperform the vanilla GNN models as well as the ones trained with structure-oriented augmentations by large margins. Utilizing the GCN as the backbone, our methods, Aug<sub>GE</sub> and Aug<sub>PE</sub>, exhibit significant enhancements in classification accuracy—2.40% and 2.75%, on average—when compared to the best-performing baselines across six datasets. With GIN, the improvements are 5.04% and 4.69%, respectively. Secondly, we observe that traditional structure-based augmentation methods yield comparatively less effectiveness. For example, in the Fluoride dataset, all baseline augmentation methods achieve negative effects, while our methods can still beat the backbone significantly.

### 6.2. Effects of Augmentation Distribution

In Section 4, we investigated explanation-assisted data augmentation methods, and argued that performance improvements are contingent on in-distribution generation of augmented data. In this section, we analyze the effects of augmentation distributions on the model accuracy. With this set of experiments on a synthetic dataset and a real-world dataset, we aim to explore two questions: (RQ1) Can in-distribution augmentations lead to better data efficiency in graph learning? (RQ2) What are the effects of out-of-distribution augmentations on graph learning?

To evaluate the data efficiency of graph learning methods, we vary the number of training samples in the range [4, 8, 20, 40, 100, 300, 500, 700]. We sufficiently train GNN models with three settings: 1) training with the vanilla training samples, 2) training with in-distribution explanation-preserving augmentation, and 3) training with out-of-distribution explanation-preserving augmentation. For setting 2, we use the proposed augmentation method on the ground truth explanations. For setting 3, to generate OOD augmentations, we randomly add 100% edges from the BA graph for each instance on the BA-2motifs dataset. On the Benzene dataset, we randomly remove 30% edges from the

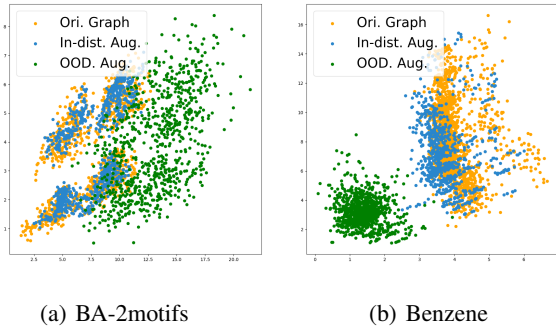


Figure 2. The visualization of original graphs, in-distributed and OOD augmentations in dataset BA-2motifs and Benzene.

non-explanation subgraphs. Visualization results on three sets of graphs are shown in Figure 2, which shows that our methods are able to generate both in-distributed and out-of-distributed augmentations for further analysis.

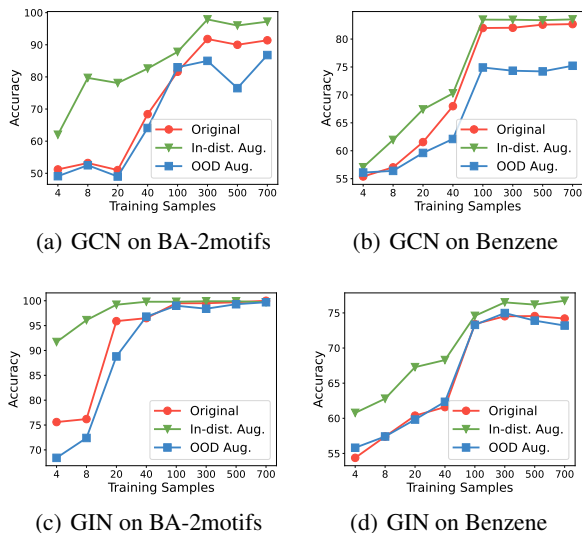


Figure 3. Effects of in-distributed and OOD augmentations on the accuracy of GCN and GIN on BA-2motifs and Benzene datasets.

We answer our research questions with accuracy performances in Figure 3. From these figures, we have the following observations. First, in-distribution augmentations significantly and consistently improve the data efficiency of both GCN and GIN in two datasets. For example, with explanation-preserving augmentations, GIN can achieve over 90% accuracy with only 4 samples in the synthetic dataset, while the performance of GIN trained with original datasets is around 75%. Second, OOD augmentations fail to improve data efficiency in most cases. Moreover, for GCN on Benzene, the OOD augmentation worsens the performance, which is aligned with our theoretical analysis.

## 7. Additional Related Work

**Explainable Graph Neural Networks.** Prior works (Ying et al., 2019; Luo et al., 2020; Yuan et al., 2020; 2022; 2021; Lin et al., 2021; Wang & Shen, 2023; Miao et al., 2023; Fang et al., 2023a; Xie et al., 2022; Ma et al., 2022) have explored various methods to provide interpretability in GNNs. Traditional methods obtain explanation by gradient, such as SA (Baldassarre & Azizpour, 2019b), Grad-CAM (Pope et al., 2019a). To develop model-agnostic explainers, perturbation-based methods, surrogate methods, and generation-based methods have been proposed. In perturbation-based methods, including GNNExplainer (Ying et al., 2019), PGExplainer (Luo et al., 2020), ReFine (Wang et al., 2021a), they generate perturbation to determine which features and subgraph structure are important. Surrogate methods (Vu & Thai, 2020; Duval & Malliaros, 2021) use a surrogate model to approximate the local prediction and use this surrogate model to generate explanations. Generation-based methods (Yuan et al., 2020; Shan et al., 2021; Wang & Shen, 2023) adopt generative models to derive instance-level or model-level explanations.

**Data Augmentation.** Data augmentation is a widely used technology in self-supervised learning (You et al., 2020; Zhu et al., 2020). A large class of graph augmentation methods can be categorized as rule-based (Wang et al., 2021b; Rong et al., 2019; Gasteiger et al., 2019; Zhao et al., 2022a) and learning-based methods (Zhao et al., 2021; Wu et al., 2022; Zhao et al., 2022b). Rule-based methods include NodeDrop (Rong et al., 2019), EdgeDrop (Feng et al., 2020), MessageDrop (Fang et al., 2023b), which randomly drop some features and information from the original graph. GraphCrop (Wang et al., 2020) and MoCL (Sun et al., 2021) randomly crop and substitute the graphs. Learning-based methods use graph neural networks to learn which edge is important, for example, ProGNN (Jin et al., 2020) learns a structural graph from a poisoned graph. GraphAug (Luo et al., 2022) proposed a reinforcement learning method to produce the label-invariant augmentations. Besides, in HalfHop (Azabou et al., 2023), authors proposed a novel graph augmentations by inserting a slow node. In (Liu et al., 2022), a local augmentation is proposed by learning the conditional distribution of the node under its neighbors.

## 8. Conclusion

Two approaches for leveraging subgraph explanations in graph learning were considered. First, explanation-assisted learning rules were considered, where the explanation subgraphs are directly fed to the learning mechanism along with labeled training samples. The sample complexity was characterized and was shown to be arbitrarily smaller than the explanation-agnostic sample complexity. Next, explanation-assisted data augmentation was considered, followed by

a generic learning rule applied to the augmented dataset. It was shown both theoretically and empirically that this may sometimes lead to better and sometimes to worse performance in terms of sample complexity, where gains are contingent on producing in-distribution augmented samples.

## References

- Agarwal, C., Queen, O., Lakkaraju, H., and Zitnik, M. Evaluating explainability for graph neural networks. *Scientific Data*, 10(1):144, 2023.
- Azabou, M., Ganesh, V., Thakoor, S., Lin, C.-H., Sathidevi, L., Liu, R., Valko, M., Veličković, P., and Dyer, E. L. Half-hop: A graph upsampling approach for slowing down message passing. In *International Conference on Machine Learning*, pp. 1341–1360. PMLR, 2023.
- Baldassarre, F. and Azizpour, H. Explainability techniques for graph convolutional networks. *arXiv preprint arXiv:1905.13686*, 2019a.
- Baldassarre, F. and Azizpour, H. Explainability techniques for graph convolutional networks. *arXiv preprint arXiv:1905.13686*, 2019b.
- Bloem-Reddy, B., Whye, Y., et al. Probabilistic symmetries and invariant neural networks. *Journal of Machine Learning Research*, 21(90):1–61, 2020.
- Borgwardt, K. M., Ong, C. S., Schönauer, S., Vishwanathan, S., Smola, A. J., and Kriegel, H.-P. Protein function prediction via graph kernels. *Bioinformatics*, 21(suppl\_1): i47–i56, 2005.
- Chen, S., Dobriban, E., and Lee, J. H. A group-theoretic framework for data augmentation. *The Journal of Machine Learning Research*, 21(1):9885–9955, 2020.
- Cohen, T. and Welling, M. Group equivariant convolutional networks. In *International conference on machine learning*, pp. 2990–2999. PMLR, 2016.
- Corso, G., Cavalleri, L., Beaini, D., Liò, P., and Veličković, P. Principal neighbourhood aggregation for graph nets. *Advances in Neural Information Processing Systems*, 33: 13260–13271, 2020.
- Debnath, A. K., Lopez de Compadre, R. L., Debnath, G., Shusterman, A. J., and Hansch, C. Structure-activity relationship of mutagenic aromatic and heteroaromatic nitro compounds. correlation with molecular orbital energies and hydrophobicity. *Journal of medicinal chemistry*, 34(2):786–797, 1991.
- Defferrard, M., Bresson, X., and Vandergheynst, P. Convolutional neural networks on graphs with fast localized spectral filtering. *Advances in neural information processing systems*, 29, 2016.
- Ding, K., Xu, Z., Tong, H., and Liu, H. Data augmentation for deep graph learning: A survey. *ACM SIGKDD Explorations Newsletter*, 24(2):61–77, 2022.
- Dobson, P. D. and Doig, A. J. Distinguishing enzyme structures from non-enzymes without alignments. *Journal of molecular biology*, 330(4):771–783, 2003.
- Duval, A. and Malliaros, F. D. Graphsvx: Shapley value explanations for graph neural networks. In *Machine Learning and Knowledge Discovery in Databases. Research Track: European Conference, ECML PKDD 2021, Bilbao, Spain, September 13–17, 2021, Proceedings, Part II 21*, pp. 302–318. Springer, 2021.
- Fang, J., Wang, X., Zhang, A., Liu, Z., He, X., and Chua, T.-S. Cooperative explanations of graph neural networks. In *Proceedings of the Sixteenth ACM International Conference on Web Search and Data Mining*, pp. 616–624, 2023a.
- Fang, T., Xiao, Z., Wang, C., Xu, J., Yang, X., and Yang, Y. Dropmessage: Unifying random dropping for graph neural networks. In *Proceedings of the AAAI Conference on Artificial Intelligence*, volume 37, pp. 4267–4275, 2023b.
- Feng, W., Zhang, J., Dong, Y., Han, Y., Luan, H., Xu, Q., Yang, Q., Kharlamov, E., and Tang, J. Graph random neural networks for semi-supervised learning on graphs. *Advances in neural information processing systems*, 33: 22092–22103, 2020.
- Gasteiger, J., Weißenberger, S., and Günnemann, S. Diffusion improves graph learning. *Advances in neural information processing systems*, 32, 2019.
- Han, X., Jiang, Z., Liu, N., and Hu, X. G-mixup: Graph data augmentation for graph classification. In *International Conference on Machine Learning*, pp. 8230–8248. PMLR, 2022.
- He, K., Zhang, X., Ren, S., and Sun, J. Deep residual learning for image recognition. In *Proceedings of the IEEE conference on computer vision and pattern recognition*, pp. 770–778, 2016.
- Huang, L., Pan, W., Zhang, Y., Qian, L., Gao, N., and Wu, Y. Data augmentation for deep learning-based radio modulation classification.
- Jin, W., Ma, Y., Liu, X., Tang, X., Wang, S., and Tang, J. Graph structure learning for robust graph neural networks. In *Proceedings of the 26th ACM SIGKDD international conference on knowledge discovery & data mining*, pp. 66–74, 2020.

- Kipf, T. N. and Welling, M. Semi-supervised classification with graph convolutional networks. In *International Conference on Learning Representations*, 2017. URL <https://openreview.net/forum?id=SJU4ayYgl>.
- Kovalevsky, V. A. The problem of character recognition from the point of view of mathematical statistics. *Character Readers and Pattern Recognition*, pp. 3–30, 1968.
- Krell, M. M. and Kim, S. K. Rotational data augmentation for electroencephalographic data. In *2017 39th Annual International Conference of the IEEE Engineering in Medicine and Biology Society (EMBC)*, pp. 471–474. IEEE, 2017.
- Krizhevsky, A., Sutskever, I., and Hinton, G. E. Imagenet classification with deep convolutional neural networks. *Advances in neural information processing systems*, 25, 2012.
- Li, Y., Zemel, R., Brockschmidt, M., and Tarlow, D. Gated graph sequence neural networks. In *Proceedings of ICLR’16*, April 2016. URL <https://www.microsoft.com/en-us/research/publication/gated-graph-sequence-neural-networks/>.
- Lin, W., Lan, H., and Li, B. Generative causal explanations for graph neural networks. In *International Conference on Machine Learning*, pp. 6666–6679. PMLR, 2021.
- Liu, S., Ying, R., Dong, H., Li, L., Xu, T., Rong, Y., Zhao, P., Huang, J., and Wu, D. Local augmentation for graph neural networks. In *International Conference on Machine Learning*, pp. 14054–14072. PMLR, 2022.
- Luo, D., Cheng, W., Xu, D., Yu, W., Zong, B., Chen, H., and Zhang, X. Parameterized explainer for graph neural network. *Advances in neural information processing systems*, 33:19620–19631, 2020.
- Luo, Y., McThrow, M., Au, W. Y., Komikado, T., Uchino, K., Maruhashi, K., and Ji, S. Automated data augmentations for graph classification. *arXiv preprint arXiv:2202.13248*, 2022.
- Ma, J., Guo, R., Mishra, S., Zhang, A., and Li, J. Clear: Generative counterfactual explanations on graphs. *Advances in Neural Information Processing Systems*, 35: 25895–25907, 2022.
- Miao, S., Liu, M., and Li, P. Interpretable and generalizable graph learning via stochastic attention mechanism. In *International Conference on Machine Learning*, pp. 15524–15543. PMLR, 2022.
- Miao, S., Luo, Y., Liu, M., and Li, P. Interpretable geometric deep learning via learnable randomness injection. In *Proceedings of the International Conference on Learning Representations (ICLR)*, 2023.
- Newman, M. *Networks*. Oxford University Press, 2nd edition, 2018.
- Pope, P. E., Kolouri, S., Rostami, M., Martin, C. E., and Hoffmann, H. Explainability methods for graph convolutional neural networks. In *Proceedings of the IEEE/CVF conference on computer vision and pattern recognition*, pp. 10772–10781, 2019a.
- Pope, P. E., Kolouri, S., Rostami, M., Martin, C. E., and Hoffmann, H. Explainability methods for graph convolutional neural networks. In *Proceedings of the IEEE/CVF conference on computer vision and pattern recognition*, pp. 10772–10781, 2019b.
- Rong, Y., Huang, W., Xu, T., and Huang, J. Dropedge: Towards deep graph convolutional networks on node classification. In *International Conference on Learning Representations*, 2019.
- Rong, Y., Bian, Y., Xu, T., Xie, W., Wei, Y., Huang, W., and Huang, J. Self-supervised graph transformer on large-scale molecular data. *Advances in Neural Information Processing Systems*, 33:12559–12571, 2020.
- Ruiz, L., Gama, F., and Ribeiro, A. Gated graph recurrent neural networks. *IEEE Transactions on Signal Processing*, 68:6303–6318, 2020.
- Sakai, Y. and Iwata, K.-i. Sharp bounds on arimoto’s conditional rényi entropies between two distinct orders. In *2017 IEEE International Symposium on Information Theory (ISIT)*, pp. 2975–2979. IEEE, 2017.
- Sánchez-Lengeling, B., Wei, J. N., Lee, B. K., Reif, E., Wang, P., Qian, W. W., McCloskey, K., Colwell, L. J., and Wiltchko, A. B. Evaluating attribution for graph neural networks. In *Advances in Neural Information Processing Systems 33: Annual Conference on Neural Information Processing Systems 2020, NeurIPS 2020, December 6-12, 2020, virtual*, 2020.
- Shan, C., Shen, Y., Zhang, Y., Li, X., and Li, D. Reinforcement learning enhanced explainer for graph neural networks. *Advances in Neural Information Processing Systems*, 34:22523–22533, 2021.
- Shao, H., Montasser, O., and Blum, A. A theory of pac learnability under transformation invariances. *Advances in Neural Information Processing Systems*, 35:13989–14001, 2022.

- Sterling, T. and Irwin, J. J. ZINC 15 - ligand discovery for everyone. *J. Chem. Inf. Model.*, 55(11):2324–2337, 2015.
- Sun, M., Xing, J., Wang, H., Chen, B., and Zhou, J. Mocl: data-driven molecular fingerprint via knowledge-aware contrastive learning from molecular graph. In *Proceedings of the 27th ACM SIGKDD Conference on Knowledge Discovery & Data Mining*, pp. 3585–3594, 2021.
- Tebbe, D. and Dwyer, S. Uncertainty and the probability of error (corresp.). *IEEE Transactions on Information theory*, 14(3):516–518, 1968.
- Vu, M. and Thai, M. T. Pgm-explainer: Probabilistic graphical model explanations for graph neural networks. *Advances in neural information processing systems*, 33:12225–12235, 2020.
- Wang, X. and Shen, H.-W. Gnninterpreter: A probabilistic generative model-level explanation for graph neural networks. In *Proceedings of the International Conference on Learning Representations (ICLR)*, 2023.
- Wang, X., Wu, Y., Zhang, A., He, X., and Chua, T.-S. Towards multi-grained explainability for graph neural networks. *Advances in Neural Information Processing Systems*, 34:18446–18458, 2021a.
- Wang, Y., Wang, W., Liang, Y., Cai, Y., and Hooi, B. Graphcrop: Subgraph cropping for graph classification. *arXiv preprint arXiv:2009.10564*, 2020.
- Wang, Y., Wang, W., Liang, Y., Cai, Y., and Hooi, B. Mixup for node and graph classification. In *Proceedings of the Web Conference 2021*, pp. 3663–3674, 2021b.
- Wu, Y.-X., Wang, X., Zhang, A., He, X., and Chua, T.-S. Discovering invariant rationales for graph neural networks. *arXiv preprint arXiv:2201.12872*, 2022.
- Xie, Y., Katariya, S., Tang, X., Huang, E., Rao, N., Subbian, K., and Ji, S. Task-agnostic graph explanations. *Advances in Neural Information Processing Systems*, 35:12027–12039, 2022.
- Xu, K., Hu, W., Leskovec, J., and Jegelka, S. How powerful are graph neural networks? In *International Conference on Learning Representations*, 2019. URL <https://openreview.net/forum?id=ryGs6iA5Km>.
- Ying, Z., Bourgeois, D., You, J., Zitnik, M., and Leskovec, J. Gnnexplainer: Generating explanations for graph neural networks. *Advances in neural information processing systems*, 32, 2019.
- You, Y., Chen, T., Sui, Y., Chen, T., Wang, Z., and Shen, Y. Graph contrastive learning with augmentations. *Advances in neural information processing systems*, 33:5812–5823, 2020.
- Yuan, H., Tang, J., Hu, X., and Ji, S. Xgnn: Towards model-level explanations of graph neural networks. In *Proceedings of the 26th ACM SIGKDD International Conference on Knowledge Discovery & Data Mining*, pp. 430–438, 2020.
- Yuan, H., Yu, H., Wang, J., Li, K., and Ji, S. On explainability of graph neural networks via subgraph explorations. In *International conference on machine learning*, pp. 12241–12252. PMLR, 2021.
- Yuan, H., Yu, H., Gui, S., and Ji, S. Explainability in graph neural networks: A taxonomic survey. *IEEE Transactions on Pattern Analysis and Machine Intelligence*, 2022.
- Yun, S., Jeong, M., Kim, R., Kang, J., and Kim, H. J. Graph transformer networks. *Advances in neural information processing systems*, 32, 2019.
- Zhao, T., Liu, Y., Neves, L., Woodford, O., Jiang, M., and Shah, N. Data augmentation for graph neural networks. In *Proceedings of the aaai conference on artificial intelligence*, volume 35, pp. 11015–11023, 2021.
- Zhao, T., Liu, G., Wang, D., Yu, W., and Jiang, M. Learning from counterfactual links for link prediction. In *International Conference on Machine Learning*, pp. 26911–26926. PMLR, 2022a.
- Zhao, T., Tang, X., Zhang, D., Jiang, H., Rao, N., Song, Y., Agrawal, P., Subbian, K., Yin, B., and Jiang, M. Autogda: Automated graph data augmentation for node classification. In *Learning on Graphs Conference*, pp. 32–1. PMLR, 2022b.
- Zheng, X., Shirani, F., Wang, T., Cheng, W., Chen, Z., Chen, H., Wei, H., and Luo, D. Towards robust fidelity for evaluating explainability of graph neural networks, 2023.
- Zhu, Y., Xu, Y., Yu, F., Liu, Q., Wu, S., and Wang, L. Deep graph contrastive representation learning. *arXiv preprint arXiv:2006.04131*, 2020.

## A. Proofs

### A.1. Proof of Proposition 3.1

Since the optimal Bayes error of predicting  $Y$  from  $\bar{G}$  is less than  $\bar{\epsilon}$ , from Fano's inequality, we must have:

$$H(Y|\bar{G}, \Psi(\bar{G})) = H(Y|\bar{G}) \leq h_b(\bar{\epsilon}), \quad (5)$$

where  $h_b(\cdot)$  denotes the binary entropy function. On the other hand, from  $(\kappa, s)$ -explainability assumption and Condition 1, we have:

$$I(Y; \bar{G}|\Psi(\bar{G})) = H(Y|\Psi(\bar{G})) - H(Y|\bar{G}) \leq \bar{\kappa}. \quad (6)$$

Combining equation 5 and equation 6, we conclude that:

$$H(Y|\Psi(\bar{G})) \leq \bar{\kappa} + h_b(\bar{\epsilon}).$$

Let  $\epsilon' \triangleq \bar{\kappa} + h_b(\bar{\epsilon})$ . From reverse Fano's inequality (Tebbe & Dwyer, 1968; Kovalevsky, 1968; Sakai & Iwata, 2017), it follows that the Bayes error of the estimation of  $Y$  based on  $\Psi(\bar{G})$  goes to zero as  $\epsilon' \rightarrow 0$ . So, there exist  $\bar{\kappa}, \bar{\epsilon}$  small enough and a classification function  $f_{exp}$  operating on  $\Psi(\bar{G})$  such that  $P(f_{exp}(\Psi(\bar{G})) \neq Y_{\bar{G}}) \leq \frac{\zeta}{2}$ . Consequently,

$$\begin{aligned} & \sum_{g_{exp}} P(\Psi(\bar{G}) = g_{exp}) P(Y_{\bar{G}'} \neq Y_{\bar{G}''} | \Psi(\bar{G}') = \Psi(\bar{G}'') = g_{exp}) \\ & \leq \sum_{g_{exp}} P(\Psi(\bar{G}) = g_{exp}) P(Y_{\bar{G}'} \neq f_{exp}(g_{exp}) \text{ or } Y_{\bar{G}''} \neq f_{exp}(g_{exp}) | \Psi(\bar{G}') = \Psi(\bar{G}'') = g_{exp}) \\ & \stackrel{(a)}{\leq} \sum_{g_{exp}} P(\Psi(\bar{G}) = g_{exp}) P(Y_{\bar{G}'} \neq f_{exp}(g_{exp}) | \Psi(\bar{G}') = \Psi(\bar{G}'') = g_{exp}) \\ & + \sum_{g_{exp}} P(\Psi(\bar{G}) = g_{exp}) P(Y_{\bar{G}''} \neq f_{exp}(g_{exp}) | \Psi(\bar{G}') = \Psi(\bar{G}'') = g_{exp}) \\ & \stackrel{(b)}{=} \sum_{g_{exp}} P(\Psi(\bar{G}') = g_{exp}) P(Y_{\bar{G}'} \neq f_{exp}(g_{exp}) | \Psi(\bar{G}') = g_{exp}) \\ & + \sum_{g_{exp}} P(\Psi(\bar{G}'') = g_{exp}) P(Y_{\bar{G}''} \neq f_{exp}(g_{exp}) | \Psi(\bar{G}'') = g_{exp}) \\ & = 2P(Y_{\bar{G}} \neq f_{exp}(\Psi(\bar{G}))) \leq \zeta, \end{aligned}$$

where in (a) we have used the union bound, and in (b) we have used the fact that  $\bar{G}'$  and  $\bar{G}''$  are independent of each other.  $\square$

### A.2. Proof of Theorem 3.5

*Proof. Proof of the upper-bound on the sample complexity:* We prove that the EA-ERM learning rule (Definition 3.2) achieves the sample complexity in the theorem statement. The proof builds upon the techniques developed for evaluating the sample complexity under transformation invariances in (Shao et al., 2022).

Fix  $m \in \mathbb{N}$ . Let  $d = VC_{EA}(\mathcal{H}, \Psi, \gamma)$ . Consider two sets  $\mathcal{T}$  and  $\mathcal{T}'$  of  $m$  independently generated labeled random graphs generated according to  $P_G$ . Let us denote the event

$$\mathcal{E}_{\mathcal{T}, \epsilon} \triangleq \{\exists f \in \mathcal{H} : err_{P_G}(\tilde{f}) \geq err_{\mathcal{T}}(f) + \epsilon\},$$

where  $err_{\mathcal{T}}(\cdot)$  denotes the empirical error over the set  $\mathcal{T}$ ,  $err_{P_G}$  denotes the statistical error with respect to  $P_G$ , and  $\tilde{f}(\cdot)$  is defined based on  $f(\cdot)$  and  $\mathcal{T}$  as in equation 3. In order to derive an upper-bound on the sample complexity, we first provide sufficient conditions on  $m$  under which  $P(\mathcal{E}_{\mathcal{T}, \epsilon}) \leq \frac{\delta}{2}$ . To this end, let us define

$$\mathcal{E}_{\mathcal{T}, \mathcal{T}', \epsilon} = \{\exists f \in \mathcal{H} : err_{\mathcal{T}'}(\tilde{f}) \geq err_{\mathcal{T}}(f) + \frac{\epsilon}{2}\}.$$

Note that:

$$P(\mathcal{E}_{\mathcal{T}, \mathcal{T}', \epsilon}) \geq P(\mathcal{E}_{\mathcal{T}, \epsilon}, \mathcal{E}_{\mathcal{T}, \mathcal{T}', \epsilon}) = P(\mathcal{E}_{\mathcal{T}, \epsilon})P(\mathcal{E}_{\mathcal{T}, \mathcal{T}', \epsilon} | \mathcal{E}_{\mathcal{T}, \epsilon}), \quad (7)$$

Consequently, to derive an upper-bound on  $P(\mathcal{E}_{\mathcal{T}, \epsilon})$  it suffices to derive a lower-bound on  $P(\mathcal{E}_{\mathcal{T}, \mathcal{T}', \epsilon} | \mathcal{E}_{\mathcal{T}, \epsilon})$  and an upper-bound on  $P(\mathcal{E}_{\mathcal{T}, \mathcal{T}', \epsilon})$ . We first derive a lower-bound on  $P(\mathcal{E}_{\mathcal{T}, \mathcal{T}', \epsilon} | \mathcal{E}_{\mathcal{T}, \epsilon})$ . Note that:

$$\begin{aligned} P(\mathcal{E}_{\mathcal{T}, \mathcal{T}', \epsilon} | \mathcal{E}_{\mathcal{T}, \epsilon}) &= P(\exists f' \in \mathcal{H} : \text{err}_{\mathcal{T}'}(\tilde{f}') \geq \text{err}_{\mathcal{T}}(f') + \frac{\epsilon}{2} | \exists f \in \mathcal{H} : \text{err}_{P_G}(\tilde{f}) \geq \text{err}_{\mathcal{T}}(f) + \epsilon) \\ &\geq P(\text{err}_{\mathcal{T}'}(\tilde{f}) \geq \text{err}_{\mathcal{T}}(f) + \frac{\epsilon}{2} | \text{err}_{P_G}(\tilde{f}) \geq \text{err}_{\mathcal{T}}(f) + \epsilon) \\ &= \sum_{(\bar{g}_i, y_i), i \in [m]} P(\mathcal{T} = \{(\bar{g}_i, y_i) | i \in [m]\}) P(\text{err}_{\mathcal{T}'}(\tilde{f}) \geq \text{err}_{\mathcal{T}}(f) + \frac{\epsilon}{2} | \text{err}_{P_G}(\tilde{f}) \geq \text{err}_{\mathcal{T}}(f) + \epsilon, \mathcal{T} = \{(\bar{g}_i, y_i) | i \in [m]\}) \end{aligned}$$

For a given realization of the training set  $\mathcal{T} = \{(\bar{g}_i, y_i), i \in [m]\}$ , let  $\text{err}_{\mathcal{T}}(f) + \epsilon$  be denoted by the (constant) variable  $c_{\mathcal{T}}$ . Then, we have:

$$P(\mathcal{E}_{\mathcal{T}, \mathcal{T}', \epsilon} | \mathcal{E}_{\mathcal{T}, \epsilon}) = \sum_{(\bar{g}_i, y_i), i \in [m]} P(\mathcal{T} = \{(\bar{g}_i, y_i) | i \in [m]\}) P(\text{err}_{\mathcal{T}'}(\tilde{f}) - c_{\mathcal{T}} \geq -\frac{\epsilon}{2} | \mathbb{E}(\text{err}_{\mathcal{T}'}(\tilde{f})) \geq c_{\mathcal{T}})$$

where we have used the fact that  $\mathcal{T}'$  is a collection of independent and identically distributed (IID) samples to conclude that  $\text{err}_{P_G}(\tilde{f}) = \mathbb{E}(\text{err}_{\mathcal{T}'}(\tilde{f}))$ . Consequently,

$$P(\mathcal{E}_{\mathcal{T}, \mathcal{T}', \epsilon} | \mathcal{E}_{\mathcal{T}, \epsilon}) \geq P(\text{err}_{\mathcal{T}'}(\tilde{f}) - \mathbb{E}(\text{err}_{\mathcal{T}'}(\tilde{f})) \geq -\frac{\epsilon}{2}),$$

where we have dropped the condition  $\mathbb{E}(\text{err}_{\mathcal{T}'}(\tilde{f})) \geq c_{\mathcal{T}}$  since  $\text{err}_{\mathcal{T}'}(\tilde{f}) - \mathbb{E}(\text{err}_{\mathcal{T}'}(\tilde{f}))$  is independent of  $\mathcal{T}$ , and used the fact that  $\sum_{(\bar{g}_i, y_i), i \in [m]} P(\mathcal{T} = \{(\bar{g}_i, y_i) | i \in [m]\}) = 1$ . Note that  $\text{err}_{\mathcal{T}'}(\tilde{f}) = \frac{1}{m} \sum_{(\bar{G}_i, Y_i) \in \mathcal{T}'} \mathbb{1}(\tilde{f}(\bar{G}_i) \neq Y_i)$  and  $\mathbb{E}(\text{err}_{\mathcal{T}'}(\tilde{f})) = P(\tilde{f}(\bar{G}_i) \neq Y_i), i \in [m]$ , where we have used the linearity of expectation. So,

$$P(\mathcal{E}_{\mathcal{T}, \mathcal{T}', \epsilon} | \mathcal{E}_{\mathcal{T}, \epsilon}) \geq P\left(\sum_{(\bar{G}_i, Y_i) \in \mathcal{T}'} (\mathbb{1}(\tilde{f}(\bar{G}_i) \neq Y_i) - P(\tilde{f}(\bar{G}_i) \neq Y_i)) \geq \frac{-m\epsilon}{2}\right) \geq 1 - e^{-\frac{2m\epsilon^2}{m}} = 1 - e^{-2m\epsilon^2},$$

where we have used the Hoeffding's inequality and the fact that  $\mathbb{1}(\tilde{f}(\bar{G}_i) \neq Y_i) \in [0, 1]$ . Hence, if  $m \geq \frac{2}{\epsilon^2}$ , then:

$$P(\mathcal{E}_{\mathcal{T}, \mathcal{T}', \epsilon} | \mathcal{E}_{\mathcal{T}, \epsilon}) \geq 1 - \frac{1}{e} \geq \frac{1}{2}. \quad (8)$$

Combining equation 7 and equation 8, we get:

$$P(\mathcal{E}_{\mathcal{T}, \mathcal{T}', \epsilon}) \geq \frac{1}{2} P(\mathcal{E}_{\mathcal{T}, \epsilon}).$$

Hence, to provide an upper-bound on  $P(\mathcal{E}_{\mathcal{T}, \epsilon})$ , it suffices to provide sufficient conditions on  $m$  such that  $P(\mathcal{E}_{\mathcal{T}, \mathcal{T}', \epsilon}) \leq \delta$ . To this end, we first introduce the notion of perturbed subset. For a given set of labeled random graphs  $\mathcal{U}$  and an element  $(\bar{G}, Y)$  in  $\mathcal{U}$ , let us define the perturbed set of  $\bar{G}$  in  $\mathcal{U}$  as  $\mathcal{O}(\bar{G} | \mathcal{U}) \triangleq \{(\bar{G}', Y) \in \mathcal{U} | \Psi(\bar{G}) \in \bar{G}'\}$ , i.e., as the set of all elements of  $\mathcal{U}$  that can be produced via explanation-preserving perturbations of  $\bar{G}$ . Furthermore, let  $n_{\mathcal{O}}(\bar{G} | \mathcal{U}) \triangleq |\mathcal{O}(\bar{G} | \mathcal{U})|$  be the number of explanation-preserving perturbations of  $\bar{G}$  in  $\mathcal{U}$ .

Next, let us define  $\mathcal{T}'' = \mathcal{T} \cup \mathcal{T}'$ . Let  $\bar{G}_1, \bar{G}_2, \dots, \bar{G}_{2m}$  be the elements of  $\mathcal{T}''$  sorted such that  $n_{\mathcal{O}}(\bar{G}_i | \mathcal{T}'') \geq n_{\mathcal{O}}(\bar{G}_j | \mathcal{T}'')$ ,  $j \leq i$ , i.e. sorted in a non-decreasing order with respect to  $n_{\mathcal{O}}(\cdot | \mathcal{T}'')$  so that there are a larger or equal number of samples which are perturbations of  $\bar{G}_i$  in  $\mathcal{T}''$  than that of  $\bar{G}_j$  for all  $j \leq i$ . We construct the sets  $\mathcal{R}_1$  and  $\mathcal{R}_2$  partitioning  $\mathcal{T}''$  as follows. Initiate  $\mathcal{R}_1 = \mathcal{R}_2 = \phi$  and  $\mathcal{T}_1'' = \mathcal{T}''$ . If  $n_{\mathcal{O}}(\bar{G}_1 | \mathcal{T}_1'') > \log^2 m$ , we add  $\mathcal{O}(\bar{G}_1 | \mathcal{T}_1'')$  to  $\mathcal{R}_1$  and construct  $\mathcal{T}_2'' = \mathcal{T}'' - \mathcal{O}(\bar{G}_1 | \mathcal{T}_1'')$ . We define  $\bar{G}^{(1)} = \bar{G}_1$  and call it the subset representative for  $\mathcal{O}(\bar{G}_1 | \mathcal{T}'')$ . Next, we arrange the elements of  $\mathcal{T}_2''$  in a non-decreasing order with respect to  $n_{\mathcal{O}}(\cdot | \mathcal{T}_2'')$  similar to the previous step. Let  $\bar{G}^{(2)}$  denote the sample with the largest  $n_{\mathcal{O}}(\cdot | \mathcal{T}_1'')$  value. If  $n_{\mathcal{O}}(\bar{G}^{(2)} | \mathcal{T}_2'') \geq \log^2 m$ , its corresponding set  $\mathcal{O}(\bar{G}^{(2)} | \mathcal{T}_2'')$  is added to  $\mathcal{R}_1$ .

This process is repeated until the  $\ell$ th step when  $n_{\mathcal{O}}(\bar{G}^{(\ell)}|\mathcal{T}_\ell)$  is less than  $\log^2 m$ . Then, we set  $\mathcal{R}_2 = \mathcal{T}_\ell$ , thus partitioning  $\mathcal{T}''$  into two sets. Loosely speaking,  $\mathcal{R}_1$  contains the samples which have more than  $\log^2 m$  of their explanation-preserving perturbations in non-overlapping subsets of  $\mathcal{T}''$ , and  $\mathcal{R}_2$  contains the samples which, after removing elements of  $\mathcal{R}_1$ , do not have more than  $\log^2 m$  of their perturbations in the other remaining samples.

We further define  $\mathcal{S}_i = \mathcal{T} \cap \mathcal{R}_i$  and  $\mathcal{S}'_i = \mathcal{T} \cap \mathcal{R}'_i, i \in \{1, 2\}$ . For any collection  $\mathcal{A} = \{(\bar{g}_i, y_i), i \in [|\mathcal{A}|]\}$  of labeled random graphs and graph classification algorithm  $f'(\cdot)$ , let  $\bar{M}_{\mathcal{A}}(f') \triangleq \frac{1}{|\mathcal{A}|} \sum_{(\bar{g}_i, y_i) \in \mathcal{A}} \mathbf{1}(f'(\bar{g}_i) \neq y_i)$  be the average number of missclassified elements of  $\mathcal{A}$  by  $f'(\cdot)$ . Then,

$$\begin{aligned} P(\mathcal{E}_{\mathcal{T}, \mathcal{T}', \epsilon}) &= P(\exists f \in \mathcal{H} : \text{err}_{\mathcal{T}'}(\tilde{f}) \geq \text{err}_{\mathcal{T}}(f) + \frac{\epsilon}{2}) \\ &\leq P(\exists f \in \mathcal{H} : \bar{M}_{\mathcal{S}'_1}(\tilde{f}) \geq \bar{M}_{\mathcal{S}_1}(\tilde{f}) + \frac{\epsilon}{4} \text{ or } \bar{M}_{\mathcal{S}'_2}(\tilde{f}) \geq \bar{M}_{\mathcal{S}_2}(\tilde{f}) + \frac{\epsilon}{4}) \\ &\leq P(\exists f \in \mathcal{H} : \bar{M}_{\mathcal{S}'_1}(\tilde{f}) \geq \bar{M}_{\mathcal{S}_1}(\tilde{f}) + \frac{\epsilon}{4}) + P(\exists f \in \mathcal{H} : \bar{M}_{\mathcal{S}'_2}(\tilde{f}) \geq \bar{M}_{\mathcal{S}_2}(\tilde{f}) + \frac{\epsilon}{4}). \end{aligned} \quad (9)$$

We upper-bound each term in equation 9 separately.

**Step 1:** Finding an upper-bound for the term  $P(\exists f \in \mathcal{H} : \bar{M}_{\mathcal{S}'_1}(\tilde{f}) \geq \bar{M}_{\mathcal{S}_1} + \frac{\epsilon}{4})$ :

We first find an upper bound for  $\ell$ . Note that by construction

- i)  $\mathcal{R}_1 = \bigcup_{i \in [\ell]} \mathcal{O}(\bar{G}^{(i)}|\mathcal{T}_i)$ ,
- ii)  $n_{\mathcal{O}}(\bar{G}^{(i)}|\mathcal{T}_i) \geq \log^2 m, i \in [\ell]$ ,
- iii)  $\mathcal{O}(\bar{G}^{(i)}|\mathcal{T}_i)$  are disjoint, and
- iv)  $|\mathcal{R}_1| \leq |\mathcal{T}''| = 2m$ .

From i) and iv), we have  $\bigcup_{i \in [\ell]} \mathcal{O}(\bar{G}^{(i)}|\mathcal{T}_i) \leq 2m$ , and from iii), we have  $\sum_{i \in [\ell]} |\mathcal{O}(\bar{G}^{(i)}|\mathcal{T}_i)| = \sum_{i \in [\ell]} n_{\mathcal{O}}(\bar{G}^{(i)}|\mathcal{T}_i) \leq 2m$ , and from ii), we conclude that  $\ell \leq \frac{2m}{\log^2 m}$ .

Next, we bound the expected number of missclassified elements of  $\mathcal{R}_1$  for which there is at least one training sample in  $\mathcal{T}$  with the same explanation subgraph. To this end, let us define:

$$\text{err}_{\mathcal{O}} \triangleq \frac{1}{m} \sum_{(\bar{G}, Y) \in \mathcal{T}''} \mathbf{1}(\tilde{f}(\bar{G}) \neq Y \wedge \exists (\bar{G}', Y') \in \mathcal{T} : \Psi(\bar{G}') \subseteq \bar{G}),$$

that is,  $\text{err}_{\mathcal{O}}$  is the fraction of elements of  $\mathcal{T}''$  which are missclassified despite the existence of at least one training sample whose explanation subgraph is a subgraph of the missclassified graph. Note that from Condition 1, from  $\Psi(\bar{G}') \subseteq \bar{G}$  we can conclude that  $\Psi(\bar{G}) = \Psi(\bar{G}')$ . Let  $\mathcal{G}_{exp}$  be the image of  $\Psi(\cdot)$ , and define

$$\text{err}_{\mathcal{O}, g_{exp}} \triangleq \frac{1}{m} \sum_{(\bar{G}'', Y_{\bar{G}''}) \in \mathcal{T}''} \mathbf{1}(\tilde{f}(\bar{G}'') \neq Y_{\bar{G}''} \wedge \exists (\bar{G}', Y') \in \mathcal{T} : \Psi(\bar{G}') = \Psi(\bar{G}'') = g_{exp}), \quad g_{exp} \in \mathcal{G}_{exp}.$$

Note that  $\text{err}_{\mathcal{O}} = \sum_{g_{exp} \in \mathcal{G}_{exp}} \text{err}_{\mathcal{O}, g_{exp}}$ . Furthermore,

$$\mathbb{E}(\text{err}_{\mathcal{O}, g_{exp}}) = \frac{1}{m} |\mathcal{T}''| P(\Psi(\bar{G}) = g_{exp}) P(Y_{\bar{G}'} \neq Y_{\bar{G}''} | \Psi(\bar{G}') = \Psi(\bar{G}'') = g_{exp}).$$

Consequently, from Proposition 3.1, we have

$$\mathbb{E}(\text{err}_{\mathcal{O}}) \leq \frac{1}{m} |\mathcal{T}''| \sum_{g_{exp}} P(\Psi(\bar{G}) = g_{exp}) P(Y_{\bar{G}'} \neq Y_{\bar{G}''} | \Psi(\bar{G}') = \Psi(\bar{G}'') = g_{exp}) \leq 2\zeta.$$

Consequently, from Hoeffding's inequality, we have  $P(\text{err}_{\mathcal{O}} \geq 4\zeta) \leq 2^{-m\zeta^2}$ . So,

$$\begin{aligned} &P(\exists f \in \mathcal{H} : \bar{M}_{\mathcal{S}'_1}(\tilde{f}) \geq \bar{M}_{\mathcal{S}_1}(\tilde{f}) + \frac{\epsilon}{4}) \\ &\leq P(\exists f \in \mathcal{H} : \bar{M}_{\mathcal{S}'_1}(\tilde{f}) \geq \bar{M}_{\mathcal{S}_1}(\tilde{f}) + \frac{\epsilon}{4}, \text{err}_{\mathcal{O}} \leq 4\zeta) + P(\text{err}_{\mathcal{O}} \geq 4\zeta) \\ &\leq P(\exists f \in \mathcal{H} : \bar{M}_{\mathcal{S}'_1}(\tilde{f}) \geq \bar{M}_{\mathcal{S}_1}(\tilde{f}) + \frac{\epsilon}{4}, \text{err}_{\mathcal{O}} \leq 4\zeta) + 2^{-m\zeta^2} \\ &\leq P(\exists f \in \mathcal{H} : \bar{M}_{\mathcal{S}'_1}(\tilde{f}) \geq \frac{\epsilon}{4}, \text{err}_{\mathcal{O}} \leq 4\zeta) + 2^{-m\zeta^2} \end{aligned}$$

Let  $\mathcal{A}$  be the set of indices of  $\mathcal{O}(\bar{G}^{(i)}|\mathcal{T}_i)$  which contain at least one sample which is misclassified by  $\tilde{f}$ . Note that since  $\text{err}_{\mathcal{O}}(\mathcal{T}) \leq 4\zeta$ , at most  $4\zeta m$  of the elements in  $\cup_{i \in [\ell]} \mathcal{O}(\bar{G}^{(i)}|\mathcal{T}_i)$  can be in  $\mathcal{T}$  and the rest must be in  $\mathcal{T}'$ . Since  $\mathcal{T}$  and  $\mathcal{T}'$  are generated identically, each element of  $\mathcal{T}''$  is in  $\mathcal{T}$  or  $\mathcal{T}'$  with equal probability, i.e., with probability equal to  $\frac{1}{2}$ .

Let  $\mathcal{I} \subseteq [\ell]$  be the set of indices of  $\mathcal{O}(\bar{G}^{(i)}|\mathcal{T}_i)$  which have at least one misclassified element. If  $|\mathcal{I}| = i$ , then  $|\cup_{j \in \mathcal{I}} \mathcal{O}(\bar{G}^{(j)}|\mathcal{T}_j)| \geq \max(i \log^2 m, \frac{m\epsilon}{4})$ , by construction. The probability that at most  $4\zeta m$  of these elements are in  $\mathcal{T}$  is upper bounded by:

$$\begin{aligned}
 & P(\exists f \in \mathcal{H} : \bar{M}_{S_1}(\tilde{f}) \geq \frac{\epsilon}{4}, \text{err}_{\mathcal{O}} \leq 4\zeta) \\
 &= P(|\cup_{j \in \mathcal{I}} \mathcal{O}(\bar{G}^{(j)}|\mathcal{T}_j) \cap \mathcal{T}| \leq 4\zeta m, |\cup_{j \in \mathcal{I}} \mathcal{O}(\bar{G}^{(j)}|\mathcal{T}_j) \cap \mathcal{T}'| \geq \frac{m\epsilon}{4}) \\
 &\stackrel{(a)}{\leq} \sum_{i=1}^{\ell} \binom{\frac{2m}{\log^2 m}}{i} \sum_{j=1}^{4\zeta m} \binom{\max(i \log^2 m, \frac{m\epsilon}{4})}{j} 2^{-\max(i \log^2 m, \frac{m\epsilon}{4})} \\
 &\leq \sum_{i=1}^{\ell} \binom{\frac{2m}{\log^2 m}}{i} 4\zeta m \binom{\max(i \log^2 m, \frac{m\epsilon}{4})}{4\zeta m} 2^{-\max(i \log^2 m, \frac{m\epsilon}{4})} \\
 &\leq \sum_{i=1}^{\ell} \binom{\frac{2m}{\log^2 m}}{i} 2^{-\max(i \log^2 m, \frac{m\epsilon}{4}) + 4\zeta m \log \max(i \log^2 m, \frac{m\epsilon}{4}) + \log m} \\
 &= \sum_{i \in [1, \frac{m\epsilon}{4 \log^2 m}]} \binom{\frac{2m}{\log^2 m}}{i} 2^{-\frac{m\epsilon}{4} + 4\zeta m \log \frac{m\epsilon}{4} + \log m} + \sum_{i \in [\frac{m\epsilon}{4 \log^2 m}, \ell]} \binom{\frac{2m}{\log^2 m}}{i} 2^{-i \log^2 m + 4\zeta m \log(i \log^2 m) + \log m} \\
 &\stackrel{(b)}{\leq} \frac{m\epsilon}{4 \log^2 m} \binom{\frac{2m}{\log^2 m}}{\frac{m\epsilon}{4 \log^2 m}} 2^{-\frac{m\epsilon}{8}} + \ell \max_{i \in [\ell]} \binom{\frac{2m}{\log^2 m}}{i} 2^{-\frac{1}{2} i \log^2 m},
 \end{aligned}$$

where in (a) we have used the union bound and in (b) we have used the fact that  $\epsilon \geq 32\zeta$ . Consequently,

$$\begin{aligned}
 & P(\exists f \in \mathcal{H} : \bar{M}_{S_1}(\tilde{f}) \geq \bar{M}_{S_1}(\tilde{f}) + \frac{\epsilon}{4}) \leq \frac{m\epsilon}{4 \log^2 m} \binom{\frac{2m}{\log^2 m}}{\frac{m\epsilon}{4 \log^2 m}} 2^{-\frac{m\epsilon}{8}} + \ell \max_{i \in [\ell]} \binom{\frac{2m}{\log^2 m}}{i} 2^{-\frac{1}{2} i \log^2 m} \\
 &\leq 2^{-\frac{m\epsilon}{16}} + \frac{2m}{\log^2 m} \max_{i \in [\ell]} 2^{-\frac{1}{2} i \log^2 m + i \log 2m} \leq 2^{-\frac{m\epsilon}{16}} + \frac{2m}{\log^2 m} 2^{-\frac{m\epsilon}{32} \log^2 m} \leq 2^{-\frac{m\epsilon}{32}}.
 \end{aligned}$$

So,

$$P(\exists f \in \mathcal{H} : \bar{M}_{S_1}(\tilde{f}) \geq \frac{\epsilon}{4}, \text{err}_{\mathcal{O}} \leq 4\zeta) \leq 2^{-\frac{\epsilon m}{32}} + 2^{-m\zeta^2} \leq 2 \cdot 2^{-\frac{\epsilon m}{32}},$$

where we have used the fact that  $1 \geq \epsilon \geq 32\zeta$ .

**Step 2:** Finding an upper-bound for the term  $P(\exists f \in \mathcal{H} : \bar{M}_{S_2}(\tilde{f}) \geq \bar{M}_{S_2}(\tilde{f}) + \frac{\epsilon}{4})$ :

By definition of  $VC_{EA}(\mathcal{H}, \Psi)$ , the number of points in  $\mathcal{R}_2$  which can be shattered by  $\mathcal{H}$  is at most  $d \log^2 m$ , where  $d \triangleq VC_{EA}(\mathcal{H}, \Psi)$ . Let  $\mathcal{K}$  be the set of all possible ways to labeling  $\mathcal{T}''$  by  $\mathcal{H}$ . Then,  $|\mathcal{K}| \leq \sum_{i=0}^{d \log^2(m)} \binom{2m}{i} \leq (\frac{2em}{d})^{d \log^2(m)}$  by Sauer's lemma. On the other hand:

$$\begin{aligned}
 & P(\exists f \in \mathcal{H} : \bar{M}_{S_2}(\tilde{f}) \geq \bar{M}_{S_2}(\tilde{f}) + \frac{\epsilon}{4}) \leq \sum_{K \in \mathcal{K}} P(\bar{M}_{S_2} \geq \mathbb{E}(\bar{M}_{S_2}) + \frac{\epsilon}{8} \text{ or } \bar{M}_{S_2} \leq \mathbb{E}(\bar{M}_{S_2}) - \frac{\epsilon}{8} | K) \\
 &\leq (\frac{2em}{d})^{d \log^2(m)} (P(\bar{M}_{S_2} \geq \mathbb{E}(\bar{M}_{S_2}) + \frac{\epsilon}{8} | K) + P(\bar{M}_{S_2} \leq \mathbb{E}(\bar{M}_{S_2}) - \frac{\epsilon}{8} | K)) \\
 &\stackrel{(a)}{\leq} 2 (\frac{2em}{d})^{d \log^2(m)} e^{-2m(\frac{\epsilon}{8})^2} \leq e^{-\frac{m\epsilon^2}{32} + d \log^2(m) \ln \frac{2em}{d}},
 \end{aligned}$$

where we have used Hoeffding's inequality in (a). Taking  $m > \frac{32}{\epsilon^2} (d \log^2(m) \ln(\frac{2em}{d}) + \ln(\frac{8}{\delta})) + \frac{32}{\epsilon} \log(\frac{8}{\delta})$ , we get  $P(\mathcal{E}_{\mathcal{T}, \frac{\epsilon}{2}}) \leq 2P(\mathcal{E}_{\mathcal{T}, \mathcal{T}', \frac{1}{2}\epsilon}) \leq 2(\frac{\delta}{8} + \frac{\delta}{8}) = \delta$ . Let  $f^*$  be the statistically optimal graph classifier in  $\mathcal{H}$ , and let  $\tilde{f}$  be the

EA-ERM output, and let the corresponding classifier minimizing the empirical risk on the augmented dataset be denoted by  $f$ . Then,

$$P(\text{err}_{P_G}(\tilde{f}) \geq \text{err}_{P_G}(f^*) + \epsilon) \quad (10)$$

$$\leq P(\text{err}_{P_G}(\tilde{f}) \geq \text{err}_{\mathcal{T}}(f) + \frac{1}{2}\epsilon \text{ or } \text{err}_{\mathcal{T}}(f) > \text{err}_{\mathcal{T}}(f^*) \text{ or } \text{err}_{\mathcal{T}}(f^*) \geq \text{err}_{P_G}(f^*) + \frac{1}{2}\epsilon) \quad (11)$$

$$\leq P(\text{err}_{P_G}(\tilde{f}) \geq \text{err}_{\mathcal{T}}(f) + \frac{1}{2}\epsilon) + P(\text{err}_{\mathcal{T}}(f) > \text{err}_{\mathcal{T}}(f^*)) + P(\text{err}_{\mathcal{T}}(f^*) \geq \text{err}_{P_G}(f^*) + \frac{1}{2}\epsilon) \quad (12)$$

$$\leq P(\mathcal{E}_{\mathcal{T}, \frac{\epsilon}{2}}) + 0 + \frac{\delta}{2} \leq \frac{\delta}{2} + \frac{\delta}{2} = \delta, \quad (13)$$

where in equation 12 we have used the union bound, and in equation 13 we have used Hoeffding’s inequality to conclude that  $P(\text{err}_{\mathcal{T}}(f^*) \geq \text{err}_{P_G}(f^*) + \frac{1}{2}\epsilon) \leq \frac{\delta}{2}$  and the definition of EA-ERM to conclude that  $P(\text{err}_{\mathcal{T}}(f) > \text{err}_{\mathcal{T}}(f^*)) = 0$ . Consequently,

$$m_{EA}(\epsilon, \delta, \zeta; \mathcal{H}, \Psi) = O\left(\frac{d}{\epsilon^2} \log^2 d + \frac{1}{\epsilon^2} \ln\left(\frac{1}{\delta}\right)\right)$$

Note that a lower-bound on sample complexity which is tight with respect to the above upper-bound follows by standard arguments. We provide an outline of the proof in the following. Let us take  $\zeta = 0$ , and let the instance space be such that for each element of the image of the explanation function, there is only one sample with non-zero probability such that the set of probable inputs are shattered by  $\mathcal{H}$ . Note that such a set of probable inputs always exists by definition of  $VC_{EA}(\mathcal{H}, \Psi)$ . In that case, it is straightforward to see that the sample complexity is the same for generic and explanation-assisted learning rules (since the explanation does not provide any additional information as for each explanation, there is only one probable input) and the lower-bound follows.  $\square$

## B. Detailed Experimental Setup

Our experiments were conducted on a Linux system equipped with eight NVIDIA A100 GPUs, each possessing 40GB of memory. We use CUDA version 11.3, Python version 3.7.16, and Pytorch version 1.12.1.

### B.1. Datasets

In our empirical experiments, we use a benchmark synthetic dataset and 6 real-life datasets.

- **BA-2motifs** (Luo et al., 2020) dataset includes 1,000 synthetic graphs created from the basic Barabasi-Albert (BA) model. This dataset is divided into two different categories: half of the graphs are associated with ‘house’ motifs, while the other half are integrated with five-node circular motifs. The labels of these graphs depends on the specific motif they incorporate.
- **MUTAG** (Debnath et al., 1991) dataset comprises 2,951 molecular graphs, divided into two classes according to their mutagenic effects on the Gram-negative bacterium *S. Typhimurium*. Functional groups  $NO_2$  and  $NH_2$  are considered as ground truth explanations for positive samples (Luo et al., 2020).
- **Benzene** (Sánchez-Lengeling et al., 2020) is a dataset of 12,000 molecular graphs from the ZINC15 database (Sterling & Irwin, 2015). The graphs are divided into two classes based on whether they have a benzene ring or not. If a molecule has more than one benzene ring, each ring is a separate explanation.
- **Fluoride** (Sánchez-Lengeling et al., 2020) dataset contains 8,671 molecular graphs, divided into two classes based on whether they have both a fluoride and a carbonyl group or not. The ground truth explanations are based on the specific combinations of fluoride atoms and carbonyl functional groups found in each molecule.
- **Alkane** (Sánchez-Lengeling et al., 2020) is a dataset of 4,326 molecular graphs, divided into two classes. A positive sample is a molecule with an unbranched alkane and a carbonyl group.

- **D&D** (Dobson & Doig, 2003) comprises 1,178 protein structures. proteins are depicted as graphs where each node represents an amino acid. Nodes are interconnected by an edge if the amino acids are within 6 Angstroms of each other. Protein structures into binary classes: enzymes and non-enzymes.
- **PROTEINS** (Dobson & Doig, 2003; Borgwardt et al., 2005) consists of 1,113 protein graphs which are generated in the same way as D&D.

The statistics of datasets are shown in Table 2. The # of explanations denotes the number of graphs with ground truth explanations.

Table 2. The detailed information of graph datasets

| Dataset    | #graphs | #nodes   | #edges      | #explanations | #classes |
|------------|---------|----------|-------------|---------------|----------|
| BA-2motifs | 1,000   | 25       | 50-52       | 1,000         | 2        |
| MUTAG      | 2,951   | 5-417    | 8-224       | 1,015         | 2        |
| Benzene    | 12,000  | 4-25     | 6-58        | 6,001         | 2        |
| Fluoride   | 8,671   | 5-25     | 8-58        | 1,527         | 2        |
| Alkane     | 4,326   | 5-25     | 8-58        | 375           | 2        |
| D&D        | 1,178   | 30-5,748 | 126 -28,534 | 0             | 2        |
| PROTEINS   | 1,113   | 4-620    | 10-2,098    | 0             | 2        |

## B.2. GNN Models

We use the same GCN model architectures and hyperparameters as (Luo et al., 2020). Specifically, For the GCN model, we embed the nodes with two GCN-Relu-BatchNorm blocks and one GCN-Relu block to learn node embeddings. Then, we adopt readout operations (Xu et al., 2019) to get graph embeddings, followed by a linear layer for graph classification. The number of neurons is set to 20 for hidden layers. For the GIN model, we replace the GCN layer with a Linear-Relu-Linear-Relu GIN layer. For the PNA model, we adopt a similar architecture in (Miao et al., 2022). We initialize the variables with the Pytorch default setting and train the models with Adam optimizer with a learning rate of  $1.0 \times 10^{-3}$ .

## B.3. Data Augmentation Baselines

- Edge Inserting: We randomly select 10% unconnected node pairs to generate the augmentation graph.
- Edge Dropping: We generate a graph by randomly removing 10% edges in the original graph.
- Node Dropping: We generate a graph by randomly dropping 10% nodes from the input graph, together with their associated edges
- Feature Dropping: We generate a graph by randomly dropping 10% features.
- Mixup: Given a labeled graph  $(\overline{G}_i, Y_i)$ , we randomly sample another labelled graph  $(\overline{G}_j, Y_j)$ . Their adjacency matrices are denoted by  $A_i$  and  $A_j$ , respectively. We generate a block diagonal matrix  $\text{diag}(A_i, A_j)$ :

$$\text{diag}(A_i, A_j) = \begin{bmatrix} A_i & 0 \\ 0 & A_j \end{bmatrix}. \tag{14}$$

The corresponding graph is denoted as  $\overline{G}^{(\text{diag})}$ . We obtain the mixup augmentation graph by randomly adding two cross-graph edges, i.e., one node from  $\overline{G}_i$  and the other from  $\overline{G}_j$ , to  $\overline{G}^{(\text{diag})}$ .

## C. Extra Experiments

In this section, we provide extensive experiments to further verify the effectiveness of our method and support our theoretical findings.

### C.1. Analysis on Distribution of Our Method

As described in Section 5, we generate augmentations by an in-distributed perturbation function  $\Pi(\cdot)$  (Algorithm 2). In this part, we empirically verify the effectiveness of our implementation in generating in-distributed augmentations. We use both GNNExplainer (Ying et al., 2019) and PGExplainer (Luo et al., 2020) to generate explanations. Two real-life datasets, Fluoride and Alkane are utilized here. For each dataset, we first pad each graph by inserting isolated nodes such that all graphs have the same size of nodes. Then, for each graph, we concatenate its adjacency matrix with the node matrix followed by a flatten operation to get a high-dimensional vector. We adopt an encoder network to embed high-dimensional vectors into a 2-D vector space. The encoder network consists of two fully connected layers, the same as the decoder network. Cross Entropy is used as the reconstruction error to train the Autoencoder model. The original graphs and augmentations are used for training. The visualization results of these original and augmentation graphs are shown in Figure 4. We observe that augmentation graphs are in-distributed in both datasets.

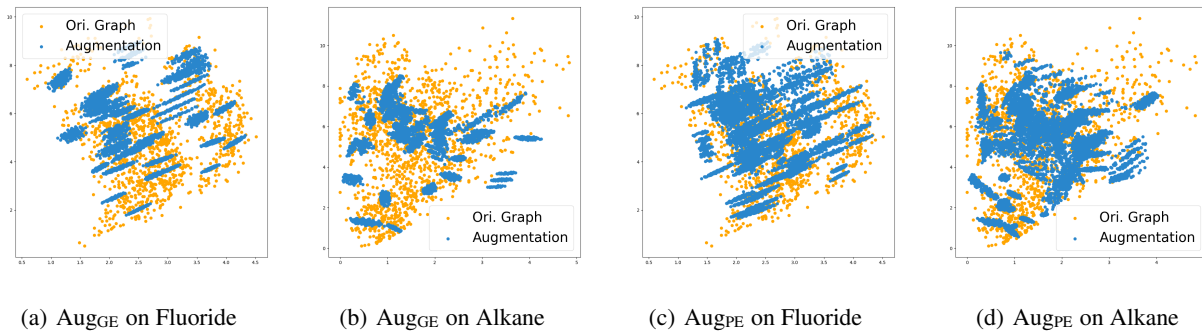


Figure 4. Visualization results of augmentations generated by Aug<sub>GE</sub> and Aug<sub>PE</sub> (best viewed in color).

### C.2. Dealing with OOD Augmentations

In this section, we conduct experiments to verify the effectiveness of our strategy that includes a hyperparameter  $\lambda$  in alleviating the negative effects of OOD graph augmentations. We select 500, 100, and 100 samples in BA-2motifs dataset as the training set, valid set, and test set, respectively. To obtain OOD augmentations, we add edges to the non-explanation subgraphs until the average node degree is not less than 17. Each training instance has 2 augmentations, and we use 3 layers GCN as the backbone. As Figure C.2 shows, in general, the accuracy decreases as the hyperparameter  $\lambda$  rises. The results show that with out-of-distribution graph augmentations, a small  $\lambda$  can alleviate the negative effects.

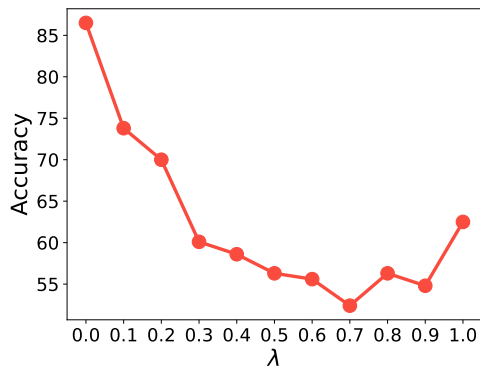


Figure 5. The effects of  $\lambda$  in tackling OOD augmentations on BA-2motifs dataset.

Table 3. Performance comparisons with 3-layer PNA trained on 50 samples. The metric is classification accuracy. The best results are shown in bold font and the second best ones are underlined.

| Dataset           | MUTAG                   | Benzene                 | Fluoride                | Alkane                  | D&D                     | PROTEINS                |
|-------------------|-------------------------|-------------------------|-------------------------|-------------------------|-------------------------|-------------------------|
| Vanilla           | 83.61 $\pm$ 4.13        | 76.72 $\pm$ 3.28        | 64.90 $\pm$ 6.88        | <u>93.60</u> $\pm$ 1.72 | 61.29 $\pm$ 5.38        | <u>64.91</u> $\pm$ 5.62 |
| Edge Inserting    | 82.35 $\pm$ 3.31        | 78.70 $\pm$ 2.29        | 64.17 $\pm$ 3.76        | 89.66 $\pm$ 4.55        | 61.81 $\pm$ 4.35        | 61.91 $\pm$ 4.44        |
| Edge Dropping     | 82.18 $\pm$ 2.68        | 77.72 $\pm$ 1.14        | 62.78 $\pm$ 1.76        | 92.31 $\pm$ 2.94        | 61.64 $\pm$ 6.22        | 60.45 $\pm$ 4.35        |
| Node Dropping     | 81.60 $\pm$ 2.39        | 78.02 $\pm$ 1.46        | 61.59 $\pm$ 3.15        | 90.77 $\pm$ 3.54        | 62.67 $\pm$ 4.28        | 61.64 $\pm$ 5.30        |
| Feature Dropping  | 81.46 $\pm$ 3.44        | 79.01 $\pm$ 1.74        | 66.63 $\pm$ 3.62        | 90.94 $\pm$ 2.94        | 62.59 $\pm$ 4.53        | 61.18 $\pm$ 3.35        |
| Mixup             | 72.21 $\pm$ 4.20        | 75.05 $\pm$ 0.93        | 61.10 $\pm$ 1.18        | 89.31 $\pm$ 2.37        | 57.45 $\pm$ 2.07        | 53.71 $\pm$ 3.36        |
| Aug <sub>GE</sub> | <b>84.73</b> $\pm$ 2.04 | <b>80.61</b> $\pm$ 0.65 | <b>68.72</b> $\pm$ 1.55 | <b>94.97</b> $\pm$ 1.46 | <b>65.43</b> $\pm$ 6.44 | 64.64 $\pm$ 5.21        |
| Aug <sub>PE</sub> | <u>84.15</u> $\pm$ 2.25 | <u>80.47</u> $\pm$ 0.82 | <u>68.60</u> $\pm$ 1.96 | 93.14 $\pm$ 2.52        | <u>63.19</u> $\pm$ 5.23 | <b>65.09</b> $\pm$ 4.62 |

### C.3. Hyper-parameter Sensitivity Studies

In this section, we show the robustness of our method with a set of hyper-parameter sensitivity studies. Two real datasets, MUTAG and Benzene, are used in this part. We choose PGExplainer to generate explanations.

As shown in Algorithm 1,  $M$  denotes the number of augmentation samples per instance. We range the values of  $M$  from 1 to 30 and show the accuracy performances of GNN models in Figure 6. Our method is robust to the selection of  $M$ .

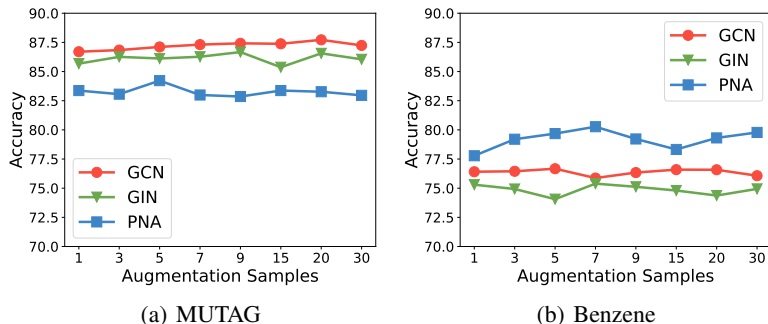


Figure 6. Hyper-parameteey study of sampling number  $M$  by using PGExplainer.

### C.4. Comparison to Baseline Data Augmentations with 3 layer PNA.

In this part, we provide the comparison of our methods to baseline data augmentations with the 3-layer PNA as the classifier. As shown in Table 3, we have similar observations with results on GCN and GIN. Our method consistently outperforms other baselines. Specifically, the improvements of Aug<sub>GE</sub> and Aug<sub>PE</sub> over the best of others are 1.99% and 1.01%, respectively.

### C.5. Comparison to Baseline Data Augmentations with Smaller Training Sizes

We show the performances of GNNs with smaller training sizes to further verify the effectiveness of our methods in improving data efficiency. We consider training sizes with 10 samples and 30 samples in this part. We use GIN in this part and keep other settings the same as Section 6.1. We also include the default setting with 50 samples for comparison.

From Table 4, we observe that Aug<sub>GE</sub> and Aug<sub>PE</sub> improves the accuracy performances by similar margins with smaller training sizes. Specifically, the improvements are 4.38% and 4.45% with 10 training samples, and 5.75% and 5.83% training samples. The results are consistent with Section 6.2, which further verify the effectiveness of our method in boosting the data efficiency for GNN training.

Table 4. Performance comparisons with 3-layer GIN trained on 10/30/50(default) samples. The metric is classification accuracy. The best results are shown in bold font and the second best ones are underlined.

|                     | Dataset          | MUTAG                            | Benzene                          | Fluoride                         | Alkane                           | D&D                              | PROTEINS                         |
|---------------------|------------------|----------------------------------|----------------------------------|----------------------------------|----------------------------------|----------------------------------|----------------------------------|
| 10 training samples | Vanilla          | 80.14 $\pm$ 5.03                 | 60.42 $\pm$ 6.10                 | 61.62 $\pm$ 2.65                 | 74.78 $\pm$ 9.24                 | 60.18 $\pm$ 5.89                 | 60.52 $\pm$ 9.50                 |
|                     | Edge Inserting   | 79.05 $\pm$ 3.85                 | 64.37 $\pm$ 4.44                 | 60.07 $\pm$ 4.84                 | 67.89 $\pm$ 12.85                | 55.45 $\pm$ 6.62                 | 58.62 $\pm$ 4.06                 |
|                     | Edge Dropping    | 74.80 $\pm$ 3.97                 | <u>65.13<math>\pm</math>2.64</u> | 60.20 $\pm$ 4.10                 | 74.65 $\pm$ 10.97                | 59.27 $\pm$ 4.65                 | 59.05 $\pm$ 5.96                 |
|                     | Node Dropping    | 76.90 $\pm$ 4.74                 | 64.88 $\pm$ 2.63                 | 59.87 $\pm$ 4.45                 | 80.14 $\pm$ 10.98                | 58.27 $\pm$ 5.07                 | 58.71 $\pm$ 7.95                 |
|                     | Feature Dropping | 75.51 $\pm$ 3.98                 | 60.95 $\pm$ 5.27                 | 61.27 $\pm$ 5.50                 | 67.08 $\pm$ 12.35                | 56.64 $\pm$ 5.16                 | 58.97 $\pm$ 6.30                 |
|                     | Mixup            | 74.35 $\pm$ 2.09                 | 51.29 $\pm$ 1.36                 | 52.25 $\pm$ 2.12                 | 62.76 $\pm$ 2.51                 | 62.27 $\pm$ 3.60                 | <b>64.66<math>\pm</math>3.74</b> |
|                     | AugGE            | 83.47 $\pm$ 2.89                 | <b>69.55<math>\pm</math>0.91</b> | <b>66.54<math>\pm</math>1.96</b> | <u>83.24<math>\pm</math>5.82</u> | <b>65.45<math>\pm</math>3.47</b> | 63.62 $\pm$ 5.48                 |
|                     | AugPE            | <b>87.48<math>\pm</math>2.26</b> | <b>69.55<math>\pm</math>0.91</b> | <u>63.00<math>\pm</math>3.49</u> | <b>84.54<math>\pm</math>6.14</b> | <u>64.91<math>\pm</math>2.34</u> | <u>63.88<math>\pm</math>3.07</u> |
| 30 training samples | Vanilla          | 81.09 $\pm$ 3.58                 | 64.37 $\pm$ 6.14                 | 66.03 $\pm$ 2.61                 | 81.41 $\pm$ 12.50                | 62.36 $\pm$ 4.85                 | 65.00 $\pm$ 7.29                 |
|                     | Edge Inserting   | 82.07 $\pm$ 3.87                 | 68.92 $\pm$ 3.07                 | 64.92 $\pm$ 3.60                 | 86.08 $\pm$ 8.59                 | 61.91 $\pm$ 5.63                 | 64.40 $\pm$ 4.03                 |
|                     | Edge Dropping    | 80.41 $\pm$ 4.02                 | 67.48 $\pm$ 4.05                 | 61.12 $\pm$ 4.10                 | 88.00 $\pm$ 7.09                 | 64.09 $\pm$ 4.01                 | 62.41 $\pm$ 5.82                 |
|                     | Node Dropping    | 81.02 $\pm$ 4.90                 | 67.93 $\pm$ 3.50                 | 60.57 $\pm$ 4.66                 | 87.61 $\pm$ 7.39                 | 64.36 $\pm$ 3.14                 | 64.22 $\pm$ 3.32                 |
|                     | Feature Dropping | 81.60 $\pm$ 4.25                 | 63.88 $\pm$ 5.67                 | 64.85 $\pm$ 6.23                 | 85.28 $\pm$ 6.12                 | 62.09 $\pm$ 5.14                 | 63.79 $\pm$ 3.99                 |
|                     | Mixup            | 72.24 $\pm$ 2.55                 | 54.28 $\pm$ 2.06                 | 52.06 $\pm$ 3.14                 | 68.31 $\pm$ 3.98                 | 56.00 $\pm$ 2.04                 | 60.95 $\pm$ 3.32                 |
|                     | AugGE            | <b>84.90<math>\pm</math>1.29</b> | <u>70.69<math>\pm</math>1.66</u> | <b>71.56<math>\pm</math>4.59</b> | <b>94.50<math>\pm</math>1.32</b> | <b>68.55<math>\pm</math>5.64</b> | <u>69.05<math>\pm</math>4.23</u> |
|                     | AugPE            | <u>84.73<math>\pm</math>1.45</u> | <b>70.81<math>\pm</math>2.30</b> | <u>71.48<math>\pm</math>3.64</u> | <u>94.28<math>\pm</math>1.42</u> | <u>68.00<math>\pm</math>6.26</u> | <b>70.17<math>\pm</math>3.50</b> |
| 50 training samples | Vanilla          | 82.52 $\pm$ 3.71                 | 67.48 $\pm$ 5.93                 | 68.55 $\pm$ 5.18                 | 85.06 $\pm$ 10.27                | 65.14 $\pm$ 4.26                 | 66.45 $\pm$ 4.01                 |
|                     | Edge Inserting   | 82.79 $\pm$ 3.21                 | 71.58 $\pm$ 2.77                 | 66.78 $\pm$ 4.04                 | 87.54 $\pm$ 10.32                | 64.74 $\pm$ 5.38                 | 65.45 $\pm$ 5.82                 |
|                     | Edge Dropping    | 81.63 $\pm$ 3.65                 | 70.46 $\pm$ 4.34                 | 62.91 $\pm$ 5.06                 | 90.29 $\pm$ 6.39                 | 66.72 $\pm$ 3.76                 | 62.73 $\pm$ 5.29                 |
|                     | Node Dropping    | 82.18 $\pm$ 3.99                 | 71.31 $\pm$ 2.71                 | 64.86 $\pm$ 4.55                 | 88.89 $\pm$ 7.00                 | 66.72 $\pm$ 2.89                 | 65.64 $\pm$ 5.38                 |
|                     | Feature Dropping | 82.72 $\pm$ 2.92                 | 70.66 $\pm$ 2.80                 | 67.58 $\pm$ 5.12                 | 83.09 $\pm$ 11.73                | 68.19 $\pm$ 4.34                 | 65.55 $\pm$ 5.00                 |
|                     | Mixup            | 74.52 $\pm$ 1.61                 | 59.00 $\pm$ 3.43                 | 51.58 $\pm$ 2.59                 | 65.80 $\pm$ 4.13                 | 58.55 $\pm$ 3.48                 | 62.16 $\pm$ 2.92                 |
|                     | AugGE            | <u>85.99<math>\pm</math>2.41</u> | <b>75.41<math>\pm</math>0.82</b> | <u>76.29<math>\pm</math>2.05</u> | <b>94.89<math>\pm</math>1.11</b> | <b>69.31<math>\pm</math>5.19</b> | <b>68.45<math>\pm</math>5.86</b> |
|                     | AugPE            | <b>86.87<math>\pm</math>1.79</b> | <u>75.39<math>\pm</math>1.03</u> | <b>76.49<math>\pm</math>1.68</b> | <u>94.77<math>\pm</math>1.14</u> | <u>67.41<math>\pm</math>2.75</u> | <u>68.09<math>\pm</math>5.52</u> |

Table 5. Accuracy performance comparison using 1 layer GNNs among datasets with 50 samples. We highlight the best and second performance by bold and underlining.

|     | Dataset           | MUTAG                            | Benzene                          | Fluoride                         | Alkane                           | D&D                              | PROTEINS                         |
|-----|-------------------|----------------------------------|----------------------------------|----------------------------------|----------------------------------|----------------------------------|----------------------------------|
| GCN | Vanilla           | 79.83 $\pm$ 3.21                 | 61.46 $\pm$ 4.39                 | 56.77 $\pm$ 4.46                 | 94.89 $\pm$ 1.65                 | 61.38 $\pm$ 6.70                 | 66.45 $\pm$ 6.95                 |
|     | Edge Inserting    | 79.42 $\pm$ 3.95                 | 65.36 $\pm$ 4.91                 | 54.84 $\pm$ 3.55                 | 92.71 $\pm$ 3.79                 | 65.26 $\pm$ 7.58                 | 62.18 $\pm$ 4.69                 |
|     | Edge Dropping     | 78.10 $\pm$ 4.50                 | 66.02 $\pm$ 4.13                 | 54.92 $\pm$ 3.47                 | 94.40 $\pm$ 1.76                 | 66.12 $\pm$ 7.20                 | 62.18 $\pm$ 4.57                 |
|     | Node Dropping     | 78.54 $\pm$ 4.24                 | 66.19 $\pm$ 4.04                 | 54.49 $\pm$ 3.43                 | 93.54 $\pm$ 2.96                 | 66.21 $\pm$ 6.11                 | 63.00 $\pm$ 5.65                 |
|     | Feature Dropping  | 79.56 $\pm$ 3.80                 | 63.92 $\pm$ 4.68                 | 54.46 $\pm$ 3.55                 | 93.11 $\pm$ 2.79                 | 66.55 $\pm$ 3.93                 | 62.91 $\pm$ 4.30                 |
|     | Mixup             | 56.67 $\pm$ 2.11                 | 50.11 $\pm$ 0.42                 | 51.94 $\pm$ 0.53                 | 61.71 $\pm$ 0.00                 | 59.09 $\pm$ 0.00                 | 56.12 $\pm$ 0.46                 |
|     | Aug <sub>GE</sub> | 84.63 $\pm$ 1.65                 | <u>69.63<math>\pm</math>2.03</u> | <b>61.81<math>\pm</math>1.54</b> | <u>95.69<math>\pm</math>1.19</u> | <u>66.98<math>\pm</math>5.38</u> | <u>66.82<math>\pm</math>4.98</u> |
|     | Aug <sub>PE</sub> | <b>85.17<math>\pm</math>1.63</b> | <b>69.64<math>\pm</math>2.07</b> | <u>61.34<math>\pm</math>1.41</u> | <b>95.86<math>\pm</math>1.14</b> | <b>67.67<math>\pm</math>5.82</b> | <b>66.91<math>\pm</math>4.83</b> |
| GIN | Vanilla           | 81.39 $\pm$ 1.71                 | 63.71 $\pm$ 3.33                 | 60.31 $\pm$ 4.52                 | 87.60 $\pm$ 5.40                 | 66.21 $\pm$ 8.48                 | 66.45 $\pm$ 3.85                 |
|     | Edge Inserting    | 81.39 $\pm$ 2.54                 | 65.95 $\pm$ 4.06                 | 60.06 $\pm$ 3.21                 | 85.46 $\pm$ 9.23                 | 65.34 $\pm$ 5.57                 | 66.18 $\pm$ 5.22                 |
|     | Edge Dropping     | 81.29 $\pm$ 1.57                 | 66.03 $\pm$ 4.06                 | 59.86 $\pm$ 3.66                 | <u>88.31<math>\pm</math>5.95</u> | 66.98 $\pm$ 3.97                 | 66.09 $\pm$ 4.81                 |
|     | Node Dropping     | 81.33 $\pm$ 1.84                 | 65.58 $\pm$ 3.46                 | 60.55 $\pm$ 2.78                 | <u>88.06<math>\pm</math>7.20</u> | 65.78 $\pm$ 4.50                 | 67.00 $\pm$ 5.69                 |
|     | Feature Dropping  | 81.12 $\pm$ 1.78                 | 65.87 $\pm$ 3.33                 | 60.45 $\pm$ 2.36                 | 85.51 $\pm$ 9.41                 | 67.07 $\pm$ 4.86                 | 62.64 $\pm$ 4.21                 |
|     | Mixup             | 70.03 $\pm$ 3.99                 | 50.19 $\pm$ 0.31                 | 51.26 $\pm$ 1.16                 | 70.29 $\pm$ 0.00                 | 54.18 $\pm$ 3.26                 | 68.53 $\pm$ 0.88                 |
|     | Aug <sub>GE</sub> | 82.45 $\pm$ 1.18                 | <u>66.52<math>\pm</math>1.55</u> | <u>64.80<math>\pm</math>1.28</u> | <b>95.09<math>\pm</math>0.98</b> | <b>72.33<math>\pm</math>3.71</b> | <u>68.09<math>\pm</math>4.09</u> |
|     | Aug <sub>PE</sub> | <b>83.16<math>\pm</math>2.10</b> | <b>66.55<math>\pm</math>1.31</b> | <b>65.10<math>\pm</math>1.39</b> | <b>95.09<math>\pm</math>0.98</b> | <u>69.22<math>\pm</math>4.28</u> | <b>68.91<math>\pm</math>4.18</b> |
| PNA | Vanilla           | 83.67 $\pm$ 4.78                 | 73.74 $\pm$ 4.57                 | 60.76 $\pm$ 4.57                 | 87.77 $\pm$ 9.73                 | 62.07 $\pm$ 3.60                 | 67.18 $\pm$ 3.76                 |
|     | Edge Inserting    | 82.07 $\pm$ 2.68                 | 75.66 $\pm$ 2.02                 | 59.55 $\pm$ 3.35                 | 89.00 $\pm$ 4.40                 | <u>64.22<math>\pm</math>4.58</u> | 65.00 $\pm$ 5.71                 |
|     | Edge Dropping     | 82.48 $\pm$ 2.97                 | 74.75 $\pm$ 2.46                 | 59.15 $\pm$ 3.71                 | 91.74 $\pm$ 3.02                 | <u>64.22<math>\pm</math>5.76</u> | 62.00 $\pm$ 8.01                 |
|     | Node Dropping     | 82.45 $\pm$ 2.36                 | 75.11 $\pm$ 1.62                 | 58.72 $\pm$ 3.38                 | 91.37 $\pm$ 2.54                 | 61.81 $\pm$ 7.44                 | 63.91 $\pm$ 8.29                 |
|     | Feature Dropping  | 82.65 $\pm$ 3.27                 | 75.60 $\pm$ 2.22                 | 61.20 $\pm$ 4.55                 | 91.03 $\pm$ 2.43                 | 65.26 $\pm$ 3.56                 | 64.64 $\pm$ 6.28                 |
|     | Mixup             | 50.00 $\pm$ 0.00                 | 70.57 $\pm$ 1.30                 | 55.30 $\pm$ 4.20                 | 38.29 $\pm$ 0.00                 | 55.45 $\pm$ 2.73                 | 50.52 $\pm$ 3.37                 |
|     | Aug <sub>GE</sub> | <b>84.39<math>\pm</math>1.55</b> | <u>77.91<math>\pm</math>1.54</u> | <b>67.32<math>\pm</math>2.68</b> | <b>94.60<math>\pm</math>1.10</b> | 63.10 $\pm$ 3.65                 | <b>69.36<math>\pm</math>4.90</b> |
|     | Aug <sub>PE</sub> | <u>84.35<math>\pm</math>1.32</u> | <b>78.12<math>\pm</math>1.37</b> | <u>66.41<math>\pm</math>2.43</u> | <u>93.74<math>\pm</math>1.12</u> | <b>66.03<math>\pm</math>3.66</b> | <u>68.55<math>\pm</math>6.03</u> |

### C.6. Comparison to Baseline Data Augmentations with 1 Layer GNNs

In this set of experiments, we analyze the effectiveness of our methods on less powerful GNNs. We reduce the GNN layers to 1 for GCN, GIN, and PNA. Other settings are kept the same as in Section 6.1. As the results are shown in Table 5, our methods with GNNExplainer and PGExplainer occupy the best and second-best positions than other six baselines, respectively. Specifically, our methods achieve 3.69%, 3.99%, 4.04% improvements with GNNExplainer and 3.89%, 3.65%, 3.27% improvements with PGExplainer on average with GCN, GIN, and PNA backbones. Similar to the results of Section 6.1, these results show that our methods can enhance the GNN performance on both powerful and less powerful GNNs.